

Conducting polyaniline nanocomposite-based paints for corrosion protection of steel

Dimitra Sazou¹ · Pravin P. Deshpande²

Received: 10 April 2016 / Accepted: 20 July 2016 / Published online: 16 December 2016
© Institute of Chemistry, Slovak Academy of Sciences 2016

Abstract The incorporation of inorganic fillers of different nature and size into conducting polyaniline (PANI)-based paint formulation extends the possibility of developing protective coatings with a self-healing capability and improved corrosion protection performance. The resulting PANI-based coatings are characterized as nanocomposite systems if the filler has nano-size dimensions. Nanofillers such as metal and metal oxide nanoparticles, clay, carbon nanotubes, graphene, and other inorganic pigments combined with PANI give rise to a variety of PANI nanocomposites with interesting properties and potential applications. The present review article concerns applications of PANI nanocomposites in steel anticorrosion technology. The advantages of PANI nanocomposite coatings over the parent polyaniline coating are highlighted. The synergistic effect of PANI and nanofiller leads to enhancement of the mechanical, physical, and chemical properties of coatings allowing the self-healing property of PANI to appear through either the anodic protection mechanism resulting in the oxide repairing at pinholes or the controlled inhibitor release mechanism by which the PANI-based nanocomposite coating liberates corrosion inhibitors (dopant ions) on demand upon the generation of a defect on the coating leading to the oxidation of the metal and hence to the reduction of PANI.

Keywords Conducting polymers · Polyaniline · Nanocomposites · Metal corrosion · Steel corrosion protection

Introduction

Conducting polymers (CPs) such as polyaniline (PANI) have been emerged as an alternative to environmentally hazardous pigments used in making traditional anticorrosive paints like those containing chromates. PANI can be an essential ingredient in smart coatings on metals preventing metal electrodisolution even in decayed areas where the metal substrate might be exposed to corrosive environments (Abu-Thabit and Makhlof 2014; Ates 2016; Deshpande et al. 2014; Khan et al. 2010; Li and Wang 2012; Spinks et al. 2002; Tallman et al. 2002). PANI is readily applied as a primer thin film on metal substrate by electrochemical deposition (Biallozor and Kupniewska 2005; Sazou 2001; Sazou and Georgolios 1997; Sazou et al. 2007). However, it is not possible to use this approach on massive engineering structures such as ships and bridges. Consequently, the chemical synthesis method (Ciric-Marjanovic 2013) has been tuned and extended towards commercial practice (Samui et al. 2003; Sathiyarayanan et al. 2009; Souza 2007; Souza et al. 2001). Use of an appropriate CP blended into epoxy resin is required for an efficient protection performance (Deshpande and Sazou 2015).

Although numerous CP-based coating systems are used in combination with epoxy resin, they have not been completely emerged in application field in which high corrosion resistance is required. A main reason for this difficulty is that while conducting polymer-based paints work as self-healing materials to initiate the oxide

✉ Dimitra Sazou
sazou@chem.auth.gr

¹ Department of Chemistry, Aristotle University of Thessaloniki, 54 124 Thessaloniki, Greece

² Department of Metallurgy and Materials Science, College of Engineering, Shivajinagar, Pune, M.S 411005, India

formation on tiny defects, in the case of large defects, generated particularly during the propagation of localized corrosion (pitting or crevice), these coatings do not protect the metal effectively for long periods of time (Rohwerder 2009). The defect-tolerance performance of CP-based coatings can be improved by adding inorganic fillers into the PANI matrix.

The incorporation of nanostructured fillers into the CP matrix leads to nanocomposite materials (Ćirić-Marjanović 2013; Gangopadhyay and De 2000). Special synthesis techniques have been suggested to optimize the incorporation of inorganic nanofillers into the CP matrix (Sen et al. 2016). The uniform distribution of nanofillers generally provides the hybrid system with properties that differ from those of individual ingredients. Using CP-based nanocomposite coatings for corrosion protection, several limitations of CPs such as processing, homogeneity, adhesion to metal surface, permeability to corrosive species, stability at elevated temperatures, and short service life can be overcome. Approaches to produce PANI nanocomposites involve in situ polymerization processes of aniline (ANI) in the presence of inorganic fillers (Fig. 1).

Several studies have demonstrated use of conducting PANI nanocomposites as effective pigments in anticorrosive coatings, e.g., see references in (Deshpande et al. 2014; Deshpande and Sazou 2015). Utilizing suitable inorganic fillers and dopant ions during the synthesis of PANI effectively modified the adhesion, high aspect ratio, barrier properties, and electrical conductivity of PANI. Metal or metal oxide nanoparticles, smectite clays (e.g., montmorillonite, MMT), carbon nanotubes (CNTs), and graphene were suggested as possible fillers in PANI nanocomposites applicable for protection of metals against corrosion. The resulted organic–inorganic hybrid nanostructured coatings seem to increase the corrosion resistance of technologically important metals such as iron (Alam et al. 2010; Anoop et al. 2013; Mostafaei and Nasirpour 2013, 2014; Mostafaei and Zolriasatein 2012; Sathiyarayanan et al. 2007b, d), aluminum (Ates and Topkaya 2015; Hosseini et al. 2011; Jafari et al. 2013; Shabani-Nooshabadi et al.

2011), magnesium (Sathiyarayanan et al. 2007a; Zhang et al. 2013) and copper (Jafari et al. 2016; Shabani-Nooshabadi and Karimian-Taheria 2015; Singh et al. 2013a).

The enhanced anticorrosion performance of PANI nanocomposite coatings containing metal and metal oxide nanoparticles has been attributed primarily to synergistic effects that improve the electrochemical corrosion property of PANI, increase the surface area available for the release of dopant ion (corrosion inhibitor) due to the nano-size filler, as in the case of TiO₂ nanoparticles (Jafari et al. 2013; Li et al. 2013b; Mahulikar et al. 2011) and enhance the cathodic protection of metals, as in the case of Zn nanoparticles where conducting PANI preserves conductance between Zn particles and metal substrate (Tuken et al. 2006).

In the case of PANI-clay nanocomposite coatings, improved protection performance has been explained on the basis of properties of clay lamellar elements (e.g., high aspect ratio, stiffness, and high in-plane strength) resulting in improved gas barrier effect, thermal stability, and mechanical strength (Soundararajah et al. 2009). Since the first report by Yeh et al. (2001), important on-going developments on preparation procedures and techniques aiming at improved protective properties of lamellar nanocomposites of PANI with a variety of layered materials have emerged. In particular, MMT in combination with PANI has been widely used for the anticorrosion protection of metals and alloys, e.g., steel (Chang et al. 2007; Kalaivasan and Shafi 2012; Olad and Rashidzadeh 2008; Yeh et al. 2007) and aluminum (Hosseini et al. 2011; Shabani-Nooshabadi et al. 2011).

This article was prepared to review the progress made in the last decade toward the direction of developing PANI nanocomposite coatings using inorganic nanostructured materials in the presence of or inside the PANI matrix for metal protection against corrosion. Emphasis is placed on PANI nanocomposite coatings used for steel protection in corrosive environments. Blends and composites of nanostructured PANI with conventional organic polymers (Pud et al. 2003) were not discussed apart, but only in conjunction with PANI-inorganic filler system when conventional polymer is one of ingredients. Suggested corrosion protection mechanisms of PANI-based coatings are briefly highlighted first, and then several examples of PANI nanocomposite coatings exhibited more effective corrosion protection of steel than neat PANI coatings are discussed. Synthesis techniques and the origin of improved anticorrosion properties of PANI nanocomposite coatings associated with special properties of the hybrid PANI nanocomposite system are outlined.

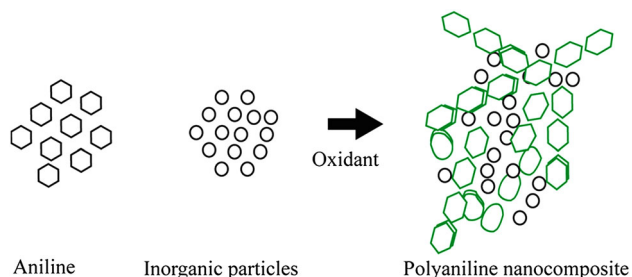


Fig. 1 Formation of the polyaniline nanocomposite from constituents using an oxidant agent

Corrosion protection mechanism induced by polyaniline-based coatings

The corrosion protection mechanism of PANI is still not fully comprehended and considerable work remains to be done toward an unanimously accepted mechanism for metal protection. PANI protection mechanism is complicated compared with that of conventional organic coatings acting mostly via a barrier effect that increases the diffusion resistance of corrosive species toward the metal substrate. Understanding the way by which PANI offers protection comprises several factors including coating formulation, corrosive environment, metal substrate, electrochemical properties, and acid–base equilibrium of PANI along with doping–dedoping process, the nature, and size of dopant ion (Dominis et al. 2003; Kinlen et al. 2002; Silva et al. 2007).

Electrochemical properties of PANI provide PANI-based coatings with self-healing and multifunctional properties. Pristine PANI exists in three different forms (Fig. 2), the completely reduced leucoemeraldine base (LEB) ($x = 0$), half-oxidized emeraldine base (EB) ($x = 0.5$), and completely oxidized pernigraniline base (PA) ($x = 1$).

PANI as LEB, EB, and PA is an insulator and only in the form of emeraldine salt (ES) exists as a conductor or rather as a semiconductor. The ES state can be achieved by proton doping (Fig. 3).

Anodic protection mechanism

Coatings containing PANI provide enhanced protection on a surface of an oxidizable metal due to the electrochemical properties of PANI. There is a general consensus that the PANI plays the role of an oxidizer either by promoting passivity through the formation of the oxide layer beneath the coating or by retarding a local corrosion process once initiation of small defects and exposition of a tiny area of the metal surface to the corrosive environment occur. The capability of PANI to maintain stainless steel in its passive state was early noticed by DeBerry (1985) introducing the idea of the anodic protection mechanism (DeBerry 1985). Wessling (1996) hypothesized and supported by a series of experimental results the self-healing capability of PANI in its ES form. It could keep the open circuit potential of a metalelectrolyte interface in anodic values, within the passive region, maintaining thereby a protective oxide layer on the metal surface. A sufficient condition to be fulfilled in this model is that oxygen reduction on the PANI-based coating can restore the polymer charge which was exhausted by metal corrosion in order for the open circuit potential to be re-established within the passive region (Wessling 1996). Reactions (1) and (2) display that the reduction of PANI results in the passivation of the metal substrate whereas the oxidized form of PANI can be

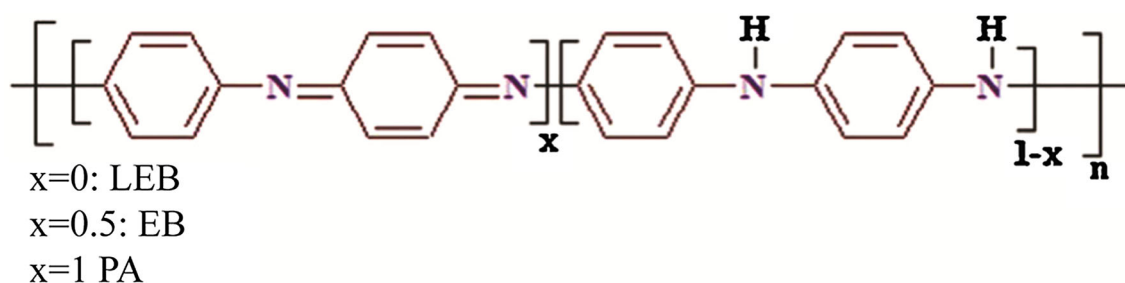


Fig. 2 Different states of pristine PANI, leucoemeraldine base (LEB) ($x = 0$, completely reduced form), emeraldine base (EB) ($x = 0.5$, half-oxidized form), and pernigraniline base (PA) ($x = 1$, completely oxidized form)

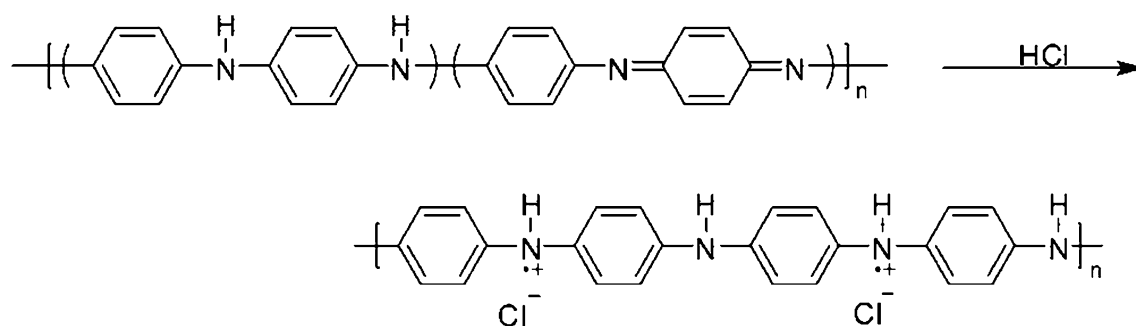
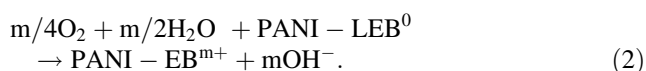
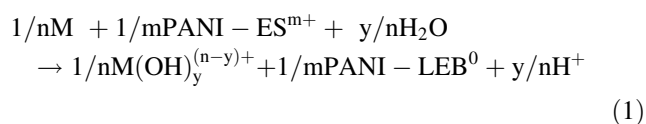
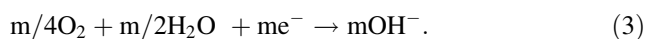


Fig. 3 Protonic doping of the emeraldine base (EB) leads to the conducting emeraldine salt (ES) of PANI

recovered by the reduction of dissolved or atmospheric oxygen:



There exist also evidences for a shift of the location of cathodic reactions due to the conductive state of PANI. For instance, the reduction of oxygen to hydroxide ions shifts from the metal surface to the PANI/electrolyte interface associated perhaps with reaction (2):



When PANI is used as a primer without a topcoat there is a high possibility for a cathodic degradation of the interfacial bonds from the metal/PANI interface and hence the delamination of PANI film from the metal substrate due to the increase of pH at the interface. Therefore, the efficacy of reactions (1)–(3) is strongly dependent on the barrier topcoat, which is expected to be impermeable to water and oxygen hindering their transport through the PANI film. The anodic protection mechanism was adequately supported by numerous evidences, particularly for metal materials exhibiting active to passive transition like iron and ferrous alloys (Deshpande and Sazou 2015).

However, contradictory experimental results and diverse opinions exist with respect to the corrosion protection properties of EB and ES states of PANI (Cecchetto et al. 2007; Dominis et al. 2003; Fang et al. 2007). Electrochemical studies on EB-coated aluminum substrates provided evidence that EB is able to promote transition of the metal to the passive state and decrease of the corrosion current depending on the EB film thickness. It was postulated that the ennobling effect of the metal substrate is mediated by the presence of ES inside the film formed by water doping of EB in the electrolyte and/or by acid–base interaction of EB with the hydrated substrate. Perhaps, this low conductivity of the film in conjunction with the low ion-permeability of EB might act beneficially in neutral environments by decreasing the hydrogen and oxygen reduction rates and thus improving the corrosion resistance of aluminum (Cecchetto et al. 2007).

In the case of ferrous metals, it is suggested that the EB form of PANI with polyurethane topcoats (amine-cured epoxy was avoided to exclude the possibility the ES form to be converted to EB due to the alkaline nature of epoxy topcoat) might provide more effective anticorrosion protection to the metal substrate. On the contrary, the effectiveness of the ES form was found to be dependent on the type of the dopant used. The dependence of the corrosion

rate on the type of dopant of PANI appears to be associated with the extent of galvanic activity between the ES and the steel substrate, which results in the reduction of PANI (Beard and Spellane 1997) manifested by the color change of the film from green to yellow (Dominis et al. 2003). Therefore, for metals, which do not exhibit active–passive transition an increase of the open circuit potential or the corrosion potential may cause an increase in corrosion current.

Controlled inhibitor release mechanism

According to the controlled inhibitor release mechanism, suitable dopant ions (selected to be corrosion inhibitors) can be released through the reduction of PANI due to metal electrodisolution at pinholes (Kendig et al. 2003; Souza 2007; Torresi et al. 2005) or ion-exchange process (Kendig and Hon 2004). The released dopant anions can either form a second physical barrier, which blocks the transport of corrosive species like aggressive anions (Kinlen et al. 2002; Souza et al. 2001) or inhibit oxygen reduction (Kendig and Hon 2004). These PANI-based coatings are also termed as smart coatings in the sense that the dopant anion (corrosion inhibitor) is released on demand, in other words, when destruction of the coating leads to metal corrosion and consequently to the PANI reduction (reactions (1) and (2)). Besides oxide formation, complexes between the inhibitor and metal ions can be produced on the metal surface resulting in additional anodic protective layers (Silva et al. 2005).

Cathodic protection mechanism

It was also observed that PANI can protect mild steel in neutral aggressive media by the contribution of a cathodic protection effect through the so-called « switching zone » mechanism (Elkais et al. 2013). Elkais et al. (2013) reported that benzoate-doped PANI shifts the corrosion potential of mild steel in 3 wt% NaCl toward negative values due to the dedoping process, reaction (1) and oxygen reduction, reaction (3). Under these conditions, the Fe electrodisolution rate is low due to the slow kinetics of reaction (3) on the PANI surface. In the LEB form of PANI, the corrosion potential is determined by the oxygen reduction on mild steel surface and the doping process, possibly by Cl^- . The electrons released during the doping process could be transferred to the metal where the oxygen reduction occurs preventing the anodic Fe electrodisolution due to the cathodic protection effect. After a partial doping of PANI, the potential shifted to less negative values and the series of the above-mentioned processes repeated. In the case of partially coated steel surfaces with benzoate-doped PANI, corrosion prevention via the

cathodic protection effect is restricted within a region located close to the PANI coating (Elkais et al. 2013).

However, there is uncertainty regarding the role of dissolved oxygen reflecting the general ambiguity for corrosion protection mechanisms by PANI (Fang et al. 2007; Nguyen et al. 2004). For instance, Li et al. (2011) pointed out the significant role of the oxygen reduction in corrosion protection by the EB form of PANI in terms of a different mechanism. In the presence of the EB coating, a dense oxide film was observed on the steel surface beneath the coating, through reactions (1) and (2), while no oxide film was formed on the exposed in 1 wt% NaCl steel area though corrosion protection was provided. This behavior was explained by the different reduction rates of O₂ on EB and bare steel. It was suggested that oxygen reduction is catalyzed on EB due to the strong activation ability of PANI on chemisorbed O₂. Thus, an oxygen concentration gradient emerges between EB-free and EB-coated areas leading to the diffusion of O₂ from the EB-free to the EB-coated area. Consequently, the depletion of O₂ results in the suppression of corrosion in the exposed EB-free area (Li et al. 2011).

Barrier protection mechanism

PANI coatings may also act as physical barriers preventing the transport of corrosive agents toward the metal substrate. In other words, an insulating PANI (EB) coating with sufficient thickness and low porosity works like a conventional barrier paint coating (Deshpande and Sazou 2015). A simple barrier effect, however, is not what is anticipated when PANI-based coatings are designed for metal protection because PANI-based coatings are intended to offer active protection. Certainly, a barrier effect works synergistically to other mechanisms originated from the electrochemical and electronic properties of PANI.

Understanding PANI protection mechanisms to a certain extent has led to a recent great effort to reinforce the corrosion protection performance of PANI-based coatings via several strategies. Among these strategies, the preparation of PANI nanocomposite coatings is regarded as a very promising approach toward the development of novel PANI-based anticorrosive coatings with enhanced activity and relatively long lasting service life. In summary, at the presence of solidnanofillers in the PANI nanocomposite system, the resulting coatings exhibit better corrosion ability due primarily to: (i) the stability of the redox activity of PANI and diminution of its degradation, (ii) improved ability of PANI to function persistently as a reservoir of inhibitor anions/dopants, which are uniformly distributed within the nanocomposite replacing chlorides in the PANI component and may be released once a defect appears and PANI is reduced, (iii) the

uniform distribution of PANI and the increased possibility of forming uniform passive layers on the metal surface, (iv) the control of the electrical conductivity of PANI influenced also by the size, functionality, and amount of doped PANI chains present in the nanocomposite system, (v) the restriction of the penetration and lengthening of the diffusion path of water and oxygen molecules through the nanocomposite coating and (vi) the enhanced mechanical stability of the coating and its high adhesion strength to the metal substrate.

By varying the nature of component materials, the synthesis technique, and reaction parameters, several physicochemical properties of PANI nanocomposite coatings can be controlled. Moreover, the versatility of techniques available for the characterization of nanocomposite materials led to the realization of new properties that have raised a wide scientific and technological interest also in other disciplines. The evaluation of the corrosion protection efficiency of PANI-based nanocomposite materials implemented on metals in the form of coatings is based primarily on electrochemical measurements, such as monitoring of the open circuit potential (OCP), potentiodynamic polarization recordings, and Tafel analysis as well as electrochemical impedance spectroscopy (EIS) carried out in corrosive environments. This series of measurements, along with weight loss measurements in some cases, has been applied in most of the studies discussed in sections following this one to assess corrosion current, or corrosion rate, corrosion potential, and resistance of PANI-based nanocomposite coatings as well as the long-term stability of coatings in corrosive media, especially in neutral chloride-containing solutions. Comparative tables composing PANI nanocomposites with different inorganic fillers applicable for corrosion protection of steel are included in Appendix.

Polyaniline–Zn nanocomposites

Zinc nanoparticles are expected to improve the barrier property of PANI coating resulting in an enhancement of its protective capability, as was observed using a combination of PANI with zinc dust (Kalendova et al. 2008). In most cases, the effective corrosion protection property of PANI–Zn hybrid materials applied on iron seems to be primarily based on a synergistic effect. Certain content of nanoparticles at a particular size is required for such a synergistic effect to be evolved bringing together barrier and redox properties of PANI–Zn nanocomposites. Adding considerably high amounts of Zn (or related ZnO, salt or complexes) in the PANI matrix may weaken the mechanical strength and the adhesion of PANI–Zn composite coatings to the substrate.

PANI–Zn nanocomposites can be readily prepared by in situ chemical polymerization of ANI in the presence of Zn nanoparticles using ammonium peroxydisulphate (APS) as oxidant in a HCl solution. The resulted PANI–Zn nanocomposite can be applied on metals in the form of coatings by the solution casting method. PANI and PANI nanocomposites were dispersed first in *N*-methyl-2-pyrrolidone (NMP). Olad and Rasouli (2010) have shown that iron samples coated with PANI–Zn (5 wt%) nanocomposite exhibit an anodic shift of the open circuit potential and decreased corrosion current in 0.1 M H₂SO₄ and 0.1 M HCl compared with iron samples coated with simple PANI (Olad and Rasouli 2010). The average size of Zn nanoparticles was ~ 80 nm. The improved corrosion protection provided by PANI–Zn nanocomposite coatings was attributed to the good barrier properties of Zn nanoparticles, and the enhancement of the electrochemical activity of PANI in the presence of Zn nanoparticles. PANI–Zn nanocomposites exhibit a higher conductivity than that of pure PANI. Similarly with PANI, Zn plays the role of a sacrificial anode resulting in a synergistic effect and thereby an efficient anticorrosion performance of PANI–Zn nanocomposite coatings on iron.

A more effective preparation method of PANI–Zn nanocomposites for industrial purposes was found to be a solution mixing method by which a solution mixing of PANI and Zn nanoparticles/particles can be prepared (Olad et al. 2011). Olad et al. (2011) found that the Zn average particle size and loading are critical factors for the improvement of the protective ability of PANI–Zn nanocomposite coatings prepared on iron by the casting method. Increasing the Zn loading increases the electrical conductivity and protective efficiency of both PANI–Zn nanocomposites and PANI–Zn composites containing Zn nano- and microparticles, respectively. Experimental results indicated a higher electrical conductivity and a better corrosion protection effect for the PANI–Zn nanocomposite coatings on iron coupons than for PANI–Zn composite coatings (Olad et al. 2011). The best corrosion protection effect in 0.1 M HCl was found for the PANI–Zn nanocomposite (4 wt%) coating. This result was associated with the good dispersion of Zn nanoparticles in the PANI matrix and hence with the low porosity of the coating and the increased tortuosity of the diffusion path of corrosive species toward the metal surface.

In an attempt to enhance the mechanical strength of PANI and take advantage of the synergistic effect of PANI and Zn in protection of iron, a hybrid thin layer coating comprising PANI–Zn nanocomposite and epoxy resin was applied on iron surfaces immersed in 0.1 M HCl (Olad et al. 2012). It was shown that the presence of both zinc nanoparticles and epoxy resin in PANI improved the overall anticorrosion performance of PANI–Zn

nanocomposite epoxy coatings on iron samples. The best anticorrosion performance evaluated on the basis of the open circuit potential and corrosion current was achieved at a loading of 4 wt% Zn nanoparticles and 3–7 wt% epoxy resin. In this PANI-based formulation, epoxy resin enhanced the mechanical and barrier properties of PANI whereas Zn nanoparticles reinforced the electrochemical anticorrosion behavior of PANI.

Polyaniline-ZnO nanocomposites

Nanostructured PANI and ZnO form a strong network in a nanocomposite coating when their content in the composite exceeds the percolation threshold (<2 wt% for nanoparticles). The combination of PANI with ZnO can hinder ionic and electronic transport processes across the film via a synergistic effect since ZnO exhibits n-type semiconductivity whereas PANI in its half-oxidized form (ES) acts as a p-type semiconductor. Therefore, p–n junction could be established in the PANI–ZnO composite, which permits electron transport only in one direction enhancing the barrier effect of the PANI–ZnO composite coating.

Patil and Radhakrishnan (2006) prepared conducting PANI-based hybrid composite coatings containing nanoparticulate ZnO in a poly(vinyl acetate) (PVAc) matrix for steel protection. The PANI was also in nanometer size, doped with dodecylbenzenesulfonic acid (DBSA). The PANI–PVAc–ZnO nanocomposite was prepared by a mixing solution method. Coatings containing both ZnO and PANI (2 wt%) in the PVAc matrix exhibit improved corrosion protection performance on steel plates immersed in saline water in comparison with the one-component PVAc coating or even the two-component PVAc–ZnO coating (Patil and Radhakrishnan 2006). Authors attributed the enhanced anticorrosion performance to the synergistic effect of PANI with PVAc and ZnO nanorods. PANI provides a physical barrier inhibiting the transfer of corrosion species to the steel surface and simultaneously assists passivation of steel either when a defect in the coating is formed and the corrosion current increases or the coating gets breached and the PANI–PVAc–ZnO composite becomes a cathode to the steel. Additionally, under these conditions, PANI can release the dopant anion (DBSA), which forming complexes with iron may also lead to the steel passivation. The release of inhibiting dopants is triggered by the reduction of PANI. The role of PANI is well supported via scanning electron microscopy (SEM) images of PANI–PVAc–ZnO coatings treated in the corrosive environment. SEM images display a uniform surface without pits such as those observed in the case of the PANI-free PVAc–ZnO coating.

In a series of studies (Mostafaei and Nasirpour 2013, 2014; Mostafaei and Zolriasatein 2012), a variety of physicochemical properties of the PANI–ZnO nanocomposites and corresponding coatings in epoxy resin were investigated upon varying the content in ZnO nanorods along with the corrosion protection ability of epoxy nanocomposite coatings. PANI filled with ZnO nanorods can be prepared by using the chemical oxidative polymerization of ANI in camphorsulfonic acid (CSA) with APS in the presence of ZnO (Mostafaei and Zolriasatein 2012). Adding ZnO nanorods as fillers in PANI matrix reduces the electrical conductivity (Mostafaei and Nasirpour 2013, 2014). The measured conductivity values of nanocomposites in comparison with those of constituents can be seen in Table 1. The decline of the electrical conductivity was attributed to interactions between PANI and ZnO nanorods as the possibility of bond formation between PANI via –NH on the surface of ZnO nanorods is enhanced resulting in the decrease of the conducting PANI:ZnO nanorods ratio (Mostafaei and Nasirpour 2014). PANI–ZnO nanocomposites show also improved thermal stability as compared to PANI assigned to strong interactions at the interface created between ZnO and PANI, though thermogravimetric analysis revealed that the decomposition trend of nanocomposites is similar to that of PANI.

Mostafaei and Nasirpour (2014) have shown that the PANI–ZnO nanocomposite combined with epoxy resin, can lead to coatings on carbon steel plates that exhibited better corrosion resistance in 3.5 wt% NaCl compared with pure epoxy and epoxy-PANI coatings (Table 1). The content of conducting materials in the epoxy binder was 2 wt% and the dry film thickness for all coatings equal to ~120 μm. Electrochemical measurements on the coated steel samples in the corrosive medium indicated that the open circuit potential shifted to anodic values, the impedance was increased and the corrosion rate was reduced in the case of PANI–ZnO nanocomposite coatings (Mostafaei and Nasirpour 2014). It was argued that ZnO nanorods, additionally to PANI, can appreciably expand the barrier effect and hence the corrosion protection performance of

the epoxy coating due to the flaky -shaped structure of PANI–ZnO nanocomposites. As was observed in SEM images (Fig. 4), the morphology of PANI exhibiting mostly agglomerates turns into a flaky structure attributed to both the presence of ZnO nanorods and doping anion (CSA).

The flaky structure of nanocomposite coatings seems to restrict the transport of water through the coating in agreement with water uptake studies, which have shown that PANI–ZnO-epoxy coatings exhibit a lesser tendency for water adsorption and penetration than PANI-epoxy coating. Additionally, adhesion tests indicated that PANI–ZnO-containing coatings exhibit an adequate adhesion to the metallic substrate. As Table 1 shows less than 5% of the coating was removed by increasing the content of ZnO nanorods. Though ZnO nanorods cannot be distinguished in SEM images (Fig. 4b), transmission electron microscopy (TEM) disclosed that PANI uniformly covers the ZnO nanorods (Fig. 5b).

On the basis of the open circuit potential monitoring with time and EIS measurements, it was found that the highest corrosion resistance of epoxy coatings containing PANI–ZnO nanocomposites appears at a content of 2 wt% in ZnO nanorods in 3.5 wt% NaCl at both 25 °C (Amir Mostafaei and Nasirpour 2014) and 65 °C (Mostafaei and Nasirpour 2013, 2014), because the presence of PANI derives an optimum barrier capability in the nanocomposite-based paint and better structural conditions for the establishment of passivity at the interface between the metal substrate and the coating. However, it should be noted that the coating resistance, R_c decreases with extending exposure of coated steel samples in 3.5 wt% NaCl, as can be seen by comparing R_c values at the beginning and after 30 days of exposure (Table 1). A further decrease of the R_c was observed by prolonging the exposure to the corrosive medium indicating the transport of Cl^- through the coating, though the R_c was sufficiently high in the case of the epoxy-PANI–ZnO nanocomposite coatings, even after 120 days of exposure in 3.5 wt% NaCl at 65 °C (Mostafaei and Nasirpour 2013, 2014).

Table 1 Electrical conductivity, σ of ZnO nanorods, CSA-doped PANI and PANI–ZnO nanocomposites along with the adhesion (measured by the % weight loss of surface material) of corresponding

epoxy coatings applied to steel samples and their resistance, R_c in 3.5 wt% NaCl at 25 °C evaluated by EIS measurements (Mostafaei and Nasirpour 2014)

Material	σ (S cm ⁻¹)	Adhesion of epoxy coatings to metal	R_c (initial) (Ω cm ²)	R_c (30 days) (Ω cm ²)
ZnO nanorods	0.016	15–35%	7×10^5	3×10^4
CSA-doped PANI	0.025	5–15%	9×10^6	1×10^6
PANI–ZnO 1 wt%	0.0068	5–15%	8×10^7	3×10^7
PANI–ZnO 2 wt%	0.0029	Less than 5%	4×10^9	3×10^9
PANI–ZnO 4 wt%	0.0014	Less than 5%	5×10^8	2×10^8

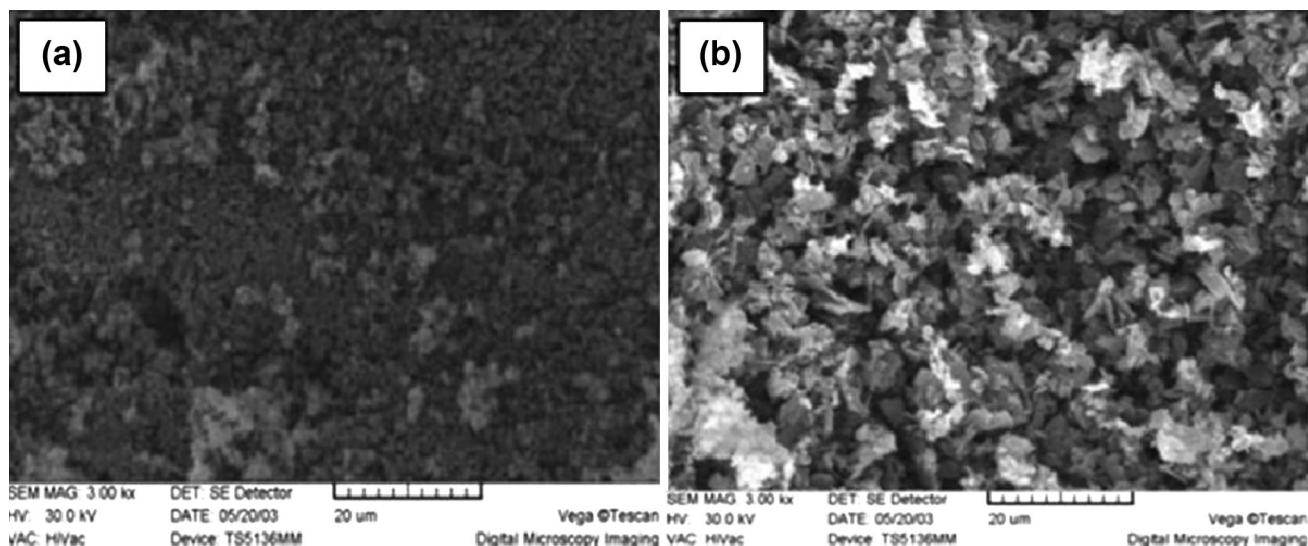


Fig. 4 SEM images of **a** CSA-doped PANI and **b** PANI–ZnO 2 wt%. Reprinted with permission from (Mostafaei and Nasirpouri 2013) *Source*: Copyright 2013 Taylor & Francis Ltd

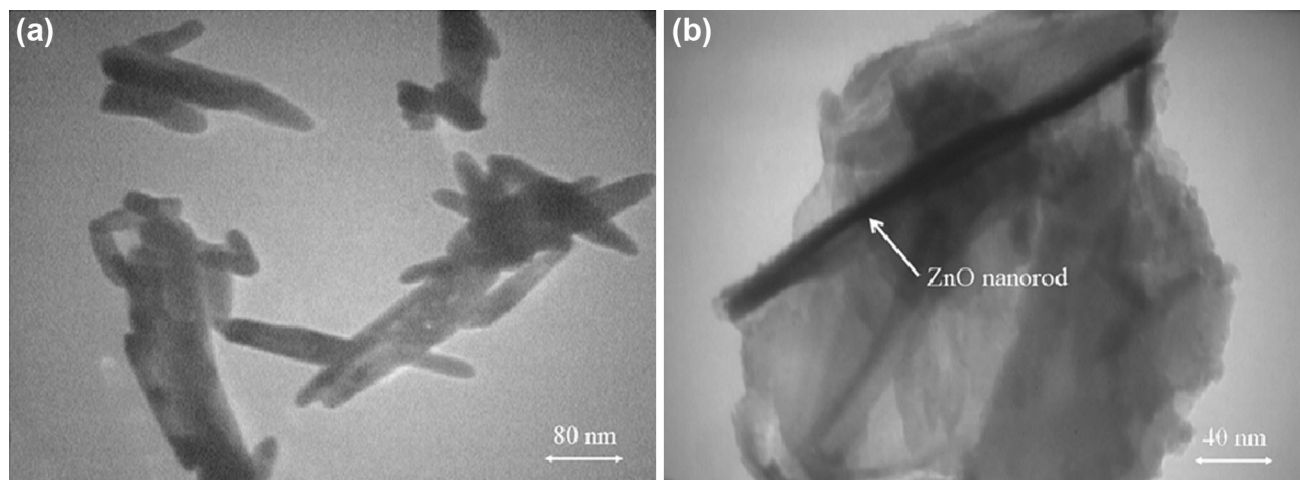
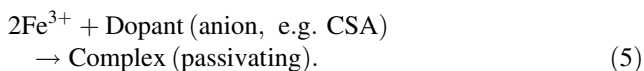
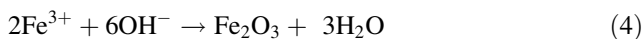


Fig. 5 TEM images of **a** ZnO nanorods with diameters ranging from 20 to 50 nm and lengths ranging from 50 to 200 nm, and **b** PANI–ZnO 2 wt% nanocomposite in which the ZnO nanorods were

In conclusion, PANI in the epoxy–PANI–ZnO nanocomposite coatings as a smart material provides a self-healing capability to the system. The PANI in epoxy coatings may be partially deprotonated resulting in the conversion of the PANI-ES to the PANI-EB due to the basic nature of the amine-cured epoxy used in coatings. It was suggested that PANI protects via anodic protection and the controlled inhibitor release mechanism by which the formation of iron oxide and iron camphorsulfonate complexes is facilitated when PANI is reduced and dopant anion is released due to the initiation of pitting corrosion:

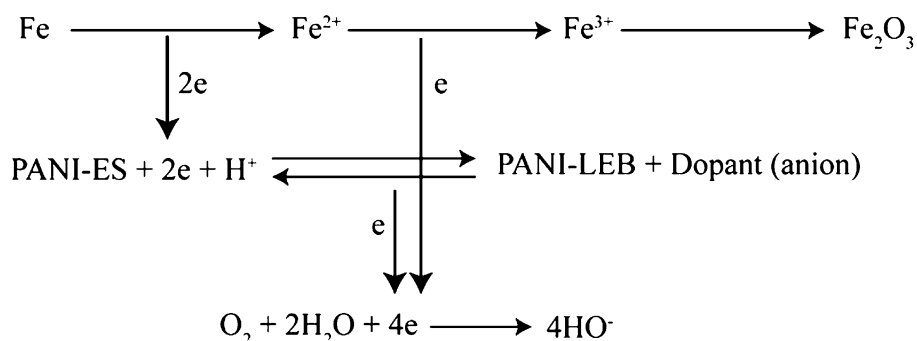


uniformly coated with PANI. Adapted with permission from (Mostafaei and Nasirpouri 2014) *Source*: Copyright 2014 Elsevier

The overall protection mechanism was described (Mostafaei and Nasirpouri 2013, 2014) as follows (Scheme 1).

The corrosion protection efficiency of PANI–ZnO nanocomposite was also examined for iron samples in 3.5 wt% NaCl in the form of coatings prepared with polyvinyl chloride (PVC) dissolved in tetrahydrofuran by a solution mixing method (Olad and Nosrati 2013). The PANI–ZnO nanocomposite with core–shell nanostructure was synthesized by in situ chemical polymerization of ANI in the presence of APS, HCl, and dispersed ZnO nanoparticles (average particle size less than 50 nm). FTIR characterization of the PANI–ZnO nanocomposite was shown that peaks related to benzenoid and quinoid rings of PANI shifted to lower wave numbers demonstrating

Scheme 1 Passivation of steel induced by conducting PANI-based nanocomposite coating



increasing electron density in PANI chains, which results in an increase of the electrical conductivity of nanocomposites, in agreement with previous studies (Alvi et al. 2010; Eskizeybek et al. 2012) but different compared to findings reported by Mostafaei and Nasirpour (2012, 2013, 2014). In latter studies, a decrease of the electrical conductivity of PANI–ZnO nanocomposites was measured. Examining the preparation approaches used in all above-mentioned studies shows that differences regarding the electrical conductivity trends of nanocomposites in the presence of ZnO nanoparticles might be associated to the different type of dopant used and perhaps to the PANI:ZnO ratio in the nanocomposite. In studies by Olad and Nosrati (2013) and Alvi et al. (2010), the polymerization was carried out in the presence of HCl, while in works by Mostafaei and Nasirpour (2012, 2013, 2014) in the presence of CSA. The type of dopant used and the level of doping influence the electron density and bond energy in the PANI chains as well as the morphology of nanocomposites. The morphology might be also affected by the structure of ZnO nanoparticles.

Corrosion tests carried out by Olad and Nosrati (2013) in 3.5 wt% NaCl by applying the three-component PVC/PANI–ZnO coating on iron coupons by casting revealed enhanced anticorrosion properties for nanocomposite coatings in comparison with pure PANI. This enhanced corrosion protection effect of the PVC/PAN–ZnO nanocomposite coating was attributed to the presence of ZnO nanoparticles that expand the barrier and electrochemical anticorrosive properties of PANI and PVC that strengthens further the barrier ability of the coating. Similarly, good corrosion protection of steel in 0.1 M HCl and 1 M NaCl was also found by Alvi et al. (2015) using PANI–ZnO nanocomposite coatings prepared by dissolving the PANI–ZnO powder in NMP (Alvi et al. 2015).

The presence of ZnO nanoparticles (with average diameter <100 nm) in the polymerization solution (sulfuric acid and aniline) during the potentiostatic deposition of the poly(*o*-phenylenediamine) (PoPDA) on austenitic stainless

steel (AISI304) was found to lead easily to PoPDA–ZnO nanocomposite coatings (Ganash 2014). The presence of ZnO nanoparticles enhanced the barrier and electrochemical properties of PoPDA and thereby supported active protection to stainless steel in 3.5 wt% NaCl for prolonging periods of time. It was suggested that ZnO nanoparticles catalyze the oxygen reduction on the PoPDA surface promoting its ability to plug pores and defects by triggering the oxide formation as soon as a pinhole appears.

In an attempt to improve the properties of PANI–ZnO nanocomposite, Alam et al. (2016) suggested a terpolymer of aniline (ANI), 2-pyridylamine (PA) and 2,3-xylydine (XY), poly(AN-*co*-PA-*co*-XY) filled with ZnO nanoparticles namely, poly(AN-*co*-PA-*co*-XY)-ZnO (Alam et al. 2016). Synthesis of the PANI-based nanocomposite was carried out through a chemical oxidative polymerization of aniline employing APS as oxidant agent. The ZnO nanoparticles, fairly dispersed into the terpolymer matrix, affect the crystalline structure of the nanocomposite. Nanocomposites of homopolymers: PANI–ZnO, poly(XY)-ZnO, and poly(PA)-ZnO were also synthesized through similar synthesis routes. The resulted compounds were deposited on mild steel specimens using solvent evaporation method with NMP as solvent and 10 wt% epoxy resin as binder. Anticorrosive properties of homopolymer nanocomposites, terpolymer, and corresponding nanocomposite coating applied on mild steel were studied in 0.1 M HCl by subjecting coated mild steel surfaces to various corrosion tests. The results revealed that after 30 days of immersion in the corrosive medium the terpolymer nanocomposite coating provided better corrosion protection in comparison to the terpolymer alone and individual homopolymer nanocomposite coatings. FTIR spectrum suggested strong interactions between terpolymer chains and ZnO nanoparticles. Prolonging the immersion of coated mild steel did not cause any significant damage to the terpolymer nanocomposite coating displaying a defect-free surface whereas the terpolymer coating was affected and ample cracks were visible on the coating surface.

Polyaniline-TiO₂ nanocomposites

PANI-TiO₂ nanocomposites can be prepared by: (i) in situ polymerization of ANI with APS as the oxidant in the presence of TiO₂ nanoparticles (usually prepared by a sol-gel method) (Radhakrishnan et al. 2009), (ii) in situ electrochemical polymerization (i.e., by cyclic voltammetry) of aniline in the presence of TiO₂ nanoparticles from 0.5 M H₂SO₄ resulting in a direct electrodeposition of the PANI-TiO₂ nanocomposite on the metal substrate (Abaci et al. 2014; Ates and Topkaya 2015), (iii) self-assembly method involved in situ polymerization of ANI and its derivatives in the presence of TiO₂ nanoparticles and salicylic acid (Mahajan and Mhaske 2012) or different surfactants (Yavuz and Aysegul 2007).

Several studies have shown that the morphology and physico-electrochemical properties of PANI-TiO₂ conducting composites differ as compared with those of the « host » PANI matrix and the « guest » TiO₂ filler (Somani et al. 1999; Su and Gan 2012). The protection efficiency of PANI-TiO₂ conducting materials is essentially improved if nanoparticles instead of microparticles of TiO₂ can be used (Sathiyarayanan et al. 2007b, d). The TiO₂ nanoparticles interacting with PANI via the formation of hydrogen bonding lead to changes in the morphology and electrical properties of PANI (Xu et al. 2005). The electrical conductivity of nanocomposites at a low TiO₂ content is greater than that of neat PANI. Upon increasing the content of TiO₂, the conductivity shows a gradual decrease. The characteristic current-voltage curve of PANI-TiO₂ heterostructure diode displays a nonlinear response which confirms that a p-n heterostructure at the interface between PANI and TiO₂ can be created (Abaci et al. 2014).

Interactions between TiO₂ particles, ANI ring substituent and dopant may also modify the morphology and properties of composites. For instance, poly(*o*-anisidine) (POA)-TiO₂ microspheres produced in the presence of salicylic acid (SA) as a dopant and APS as oxidant displayed regular spherical morphology. The spherical morphology established via the self-assembly of microspheres was assigned to the hydrogen bonding between the -OH group of SA and the amine group of POA as well as to the interactions developed between POA and TiO₂ particles. The conductivity of POA-SA-TiO₂ composite microspheres was lesser than that of the POA-SA coating (Mahajan and Mhaske 2012).

Radhakrishnan et al. (2009) prepared conducting PANI-TiO₂ nanocomposite-based coatings for the protection of stainless steel plates. PANI-TiO₂ nanocomposites of different PANI:TiO₂ ratios were synthesized chemically by in situ chemical polymerization of ANI in the presence of APS, HCl and different amounts of TiO₂ nanoparticles.

The stainless steel substrate was dip coated in a dispersion formed by mixing PANI-TiO₂ powder with polyvinyl butyral (PVB). The open circuit potential of the coated stainless steel (0.38 V_{SCE}) in 3.5 wt% NaCl shifted anodically with time. The presence of TiO₂ nanoparticles in the PANI-TiO₂ nanocomposite coating was found to be crucial in ennobling the open circuit potential and enhancing the corrosion resistance of the coated stainless steel. It was postulated that PANI as p-type semiconductor impedes electron transport, while TiO₂ as n-type semiconductor prevents the hole transport through the interface. Additionally, the charge transport from PANI to TiO₂ is hindered due to the difference in energy levels. Therefore, a synergistic effect was suggested to be responsible for the outstanding corrosion protection performance of PANI-TiO₂ nanocomposite coatings (Radhakrishnan et al. 2009).

Mahulikar et al. (2011) have observed that PANI-TiO₂ nanocomposites in epoxy binder showed superior physicochemical and mechanical properties when applied on carbon steel panels compared to plain nanoPANI-containing coatings in epoxy binder. PANI spherical nanoparticles were prepared by emulsion polymerization in the micellar solution of sodium dodecyl sulfate. Improved anticorrosion performance of PANI-TiO₂-epoxy nanocomposite coatings for carbon steel in 3.5 wt% NaCl, 5 wt% HCl, 5 wt% NaOH was rationalized via enhanced barrier property, oxide formation ability, and p-n junction effect, which contributes by inhibiting charge transport when a pinhole was formed (Mahulikar et al. 2011).

Strongly adherent core-shell PANI-TiO₂ nanocomposite films electrodeposited on a steel electrode by cyclic voltammetry from a polymerization solution containing ANI, oxalic acid solution, and TiO₂ (rutile) nanoparticles displayed superior corrosion protection effect in 1 wt% NaCl that pure PANI films (Karpakam et al. 2011). The enhanced anticorrosion performance of PANI-TiO₂ nanocomposite films was attributed to the strong interactions, perhaps hydrogen bonding, between the PANI and TiO₂ nanoparticles revealed by FTIR and XPS techniques, the high adhesion strength, homogeneity of the nanocomposite film and the stable electroactivity of PANI-TiO₂ nanocomposite films.

Interactions between the polymer and TiO₂ particles resulted in a more uniform structure of the obtained composite. Characterization of poly(2,3-dimethylaniline) (PDMA)-TiO₂ composites prepared by in situ oxidative polymerization of 2,3-dimethylaniline (DMA) in phosphoric acid medium with APS as oxidant showed that TiO₂ particles were encapsulated or entrapped into the polymer core than being simply blended or mixed up. The higher protective efficiency of PDMA-TiO₂-containing epoxy resin coatings against the corrosion of steel in 3.5 wt% NaCl in comparison with that of PANI- and PDMA-containing coatings was

attributed to a synergistic result between the electrochemical properties of PDMA, the large surface area available for the liberation of dopant due to the presence of TiO₂ nanoparticles and the increase of the barrier against the transport of corrosive species (Li et al. 2013b).

Cyclic voltammetry applied for the direct electrodeposition of PANI–TiO₂ composite on A304 stainless steel from LiClO₄-sulfuric acid solution led to PANI–TiO₂ coatings with TiO₂ nanoparticles homogeneously covered by PANI. The corrosion protection properties of PANI–TiO₂ coatings investigated in 1 M H₂SO₄ by potentiodynamic polarization and EIS measurements were noticeably enhanced in the presence of TiO₂. The protection efficiency of PANI–TiO₂ nanocomposite coating depends on the ANI:TiO₂ ratio in the polymerization solution and is promoted at a low content of TiO₂ (Abaci and Nessark 2015). The corrosion protection effect of PANI–TiO₂ coatings seems to be related to the decrease of PANI degradation and low porosity of the composite coating in the presence of TiO₂ particles.

Therefore, improvement of the barrier effect and other physico-mechanical properties of PANI–TiO₂ nanocomposite coatings, stabilization of the redox activity of PANI, enlargement of the surface area available for the release of dopant ions, and establishment of a p–n junction between PANI and TiO₂ nanoparticles to hinder charge transport once the coating is broken are all factors operating synergistically toward the enhancement of the coating protection efficiency when low amount of TiO₂ nanoparticles are encapsulated in the PANI matrix.

Polyaniline–ZrO₂ nanocomposites

ZrO₂ was widely used effectively as anticorrosion material on mild steel (Behzadnasab et al. 2011) and NiTi (Sui and Cai 2006). The combination of PANI and its derivatives with ZrO₂ might be expected to result in composite materials with improved anticorrosion properties (Gu et al. 2012). Toward this goal, ZrO₂ nanoparticles were combined with poly(*o*-toluidine) (POT) resulted in the POT–ZrO₂ nanocomposite coating (Chaudhari et al. 2007). Using cyclic voltammetry, Chaudhari et al. (2007) synthesized electrochemically, in a single step, strongly adherent poly(*o*-toluidine) (POT)–ZrO₂ coatings on mild steel from aqueous tartrate solutions of *o*-toluidine containing ZrO₂ nanoparticle. Potentiodynamic polarization and EIS measurements have shown that the inclusion of ZrO₂ nanoparticles into the polymer matrix can notably improve the corrosion properties of POT in aqueous 3 wt% NaCl. This behavior was assigned to the lower porosity of the POT–ZrO₂ nanocomposite coating that hinders the access of chlorides to the mild steel substrate. The POT–ZrO₂ nanocomposite surface was uniform displaying a pore-free and smooth morphology. It seems that either the ZrO₂

particles seal the pores in the coating or the addition of ZrO₂ changes the morphology of the POT (Chaudhari et al. 2007).

Polyaniline–CdO nanocomposites

Cadmium-containing coatings are widely used in pigments to prevent galvanic corrosion between steel and aluminum and prolong anticorrosive protection. CdO is an inorganic counterpart in the composite. Within this framework, Chaudhari et al. (2010) suggested the electrochemical synthesis of POT–CdO nanocomposite to serve as a corrosion protection coating on mild steel. Anticorrosion properties can be regulated by controlling the incorporation of CdO-nanoparticles (~18 nm) into poly(*o*-toluidine) (POT) from an aqueous tartrate solution. It was shown that the electrodeposited POT–CdO nanocomposite may function as excellent anticorrosive coating preventing initiation of localized corrosion on mild steel in 3 wt% NaCl (Chaudhari et al. 2010).

Polyaniline -ferrite nanocomposites

The combination of PANI with ferrite-type pigments was found to exhibit good protection properties against the corrosion of carbon steel (Brodinove et al. 2007). Ferrite-type pigments were first prepared by mixing oxides (ZnO) and carbonates (CaCO₃, MgCO₃) of relevant metals with iron oxide, and PANI deposition was carried out on pigment particles by oxidative polymerization of ANI. This type of PANI-ferrite-alkyd coatings demonstrated higher anticorrosive capability than PANI-alkyd coatings due to the presence of ferrite. It should be noted that PANI-alkyd coatings alone exhibited also a considerable protective effect against the corrosion of steel in aggressive environments like 5 wt% HCl, 5 wt% NaOH, and 3.5 wt% NaCl (Alam et al. 2009). PANI-alkyd coatings attract special interest in metal protection technology as they are prepared using the soya oil alkyd. Due to their unique chemical structure with unsaturation sites, epoxies, hydroxyls, esters, and other functional groups along with inherent fluidity characteristics, the vegetable oils constitute a large class of eco-friendly, low cost materials capable to be used as ingredients in paints and coatings (Alam et al. 2014).

The preparation of PANI-ferrite-alkyd coatings can be achieved by mixing a proper amount of PANI-ferrite with 10 wt% soya oil alkyd solution in xylene to attain different loadings of the nanocomposite, ranging from 0.5 to 1.5 wt% (Alam et al. 2008). The PANI in PANI-alkyd coatings was produced by emulsion polymerization employing sodium dodecyl sulfonate (Oh and Im 2002). Alam et al. (2008) have shown that the physicochemical and mechanical properties of PANI-alkyd coatings were considerably improved with increasing the loading of alkyd

in the PANI-ferrite nanocomposite. PANI-ferrite-alkyd coatings work as efficient inhibitors against the corrosion of steel in 5 wt% HCl, maintaining high resistance to corrosive ions (Alam et al. 2008). Equally effective corrosion inhibition was also observed in alkaline media for the PANI-ferrite-alkyd-coated steel. The inhibition efficiency of the composite was found to be of the order of 83% in 3.5 wt% HCl and 79% in 3.5 wt% NaOH (Alam et al. 2010). The improved inhibition efficiency of the PANI-ferrite-alkyd nanocomposite coating as compared with that of PANI-alkyd coatings was attributed to the dense, nonporous, continuous network-like structure of the nanocomposite coating.

Polyaniline-Fe₂O₃·NiO nanocomposites

There exist evidences that the 1:1 PANI-Fe₂O₃ composite coating containing phosphate as a dopant provided higher corrosion protection to steel in 3 wt% NaCl than the coatings containing only Fe₂O₃ or PANI due to the growth of a passive oxide film along with the establishment of an iron-phosphate salt film on the iron surface (Sathiyarayanan et al. 2007c). It is anticipated that the presence of Fe₂O₃ nanoparticles instead of Fe₂O₃ microparticles would provide even a better protection effect.

As was shown by Nghia and Tung (2009), PANI-Fe₂O₃·NiO nanocomposites with interesting magnetic and conductive properties can be prepared using in situ polymerization of aniline in the presence of Fe₂O₃·NiO nanoparticles synthesized by precipitation-oxidation methods. Investigations regarding the structure of the PANI-Fe₂O₃·NiO nanocomposite showed that Fe₂O₃·NiO nanoparticles were well dispersed in the PANI matrix with a uniform size ranging between 50 and 60 nm. Moreover, it was found that the saturated magnetization of the nanocomposite increases whereas its electrical conductivity decreases by increasing the Fe₂O₃·NiO content. Corrosion tests on painted steel panels in 3 wt% NaCl disclosed that the protective functioning of polyurethane paint containing PANI-Fe₂O₃·NiO nanocomposite was appreciably extended with increasing the PANI-Fe₂O₃·NiO content in paint (Nghia and Tung 2009).

Hydrophobic polyaniline-SiO₂ nanocomposites

PANI-SiO₂ composite coatings doped with dodecylbenzenesulfonic acid and blended in polystyrene exhibited enhanced corrosion protection for cold-rolled steel than PANI (Weng et al. 2012). Weng et al. (2012) assigned

this enhanced protective property to the synergistic effect of the passive oxide layer stabilized or restored by PANI on the metal surface and the barrier property of PANI-SiO₂ core-shell microspheres. Using SiO₂ particles in nano- instead of micro-size in composite coatings, the active role of PANI in corrosion protection seems to be further promoted.

Corrosion studies have shown that PANI-SiO₂ nanocomposites in the form of coatings showed enhanced protection properties ascribed to the improved electrochemical properties and uniform dispersion of PANI in the coating. PANI-SiO₂ nanocomposites can be synthesized electrochemically or chemically by in situ polymerization of ANI (Bhandari et al. 2012) as well as by emulsion polymerization (Yu et al. 2012) in the presence of properly treated SiO₂ nanoparticles. SiO₂ nanoparticles of uniform size can be obtained by a hydrolysis process of tetraethyl orthosilicate (TEOS) in the presence of aqueous ammonia followed by isolation of silicon dioxide and calcination at 823 K (Bhandari et al. 2012). Though PANI-SiO₂ hybrid coatings prepared directly from a PANI emulsion medium and TEOS via a sol-gel process provided improved barrier effect and corrosion protection, the increase of TEOS content in the PANI-SiO₂ nanocomposite caused fragility and micro-breaks in the coating which might lead to the deterioration of the anticorrosion property.

PANI-SiO₂ nanocomposites with improved hydrophobic character can be prepared by in situ chemical oxidative polymerization of ANI using APS as an oxidant in 0.2 M phosphoric acid/0.2 M perfluoro octanoic acid (PFOA). By this method, SiO₂ particles formed micelles in PFOA and ANI was adsorbed on SiO₂ nanoparticles. The polymerization process was controlled by a drop-wise addition of APS for 4–6 h at a temperature of 0–3 °C (Fig. 6). The PANI-SiO₂ can then be isolated and dried.

The powder coating method was suggested to be convenient and effective in developing hydrophobic, highly adhesive, long-lasting polymer nanocomposite coatings (Anoop et al. 2013). Hydrophobic PANI-SiO₂ nanocomposites synthesized chemically by in situ polymerization and deposited on mild steel via powder coating method exhibit improved corrosion protection performance as compared to that of PANI in 3.5 wt% NaCl. The hydrophobic character of the PANI-SiO₂ nanocomposite and the reinforcement of PANI chains due to the presence of SiO₂ nanoparticles were considered as critical factors for the anticorrosion effectiveness of these coatings (Bhandari et al. 2012). Therefore, the PANI-SiO₂ nanocomposite facilitates the formation of the passive oxide layer due to the presence of PANI and simultaneously acts as a physical barrier to prevent chloride transport to reach the metal

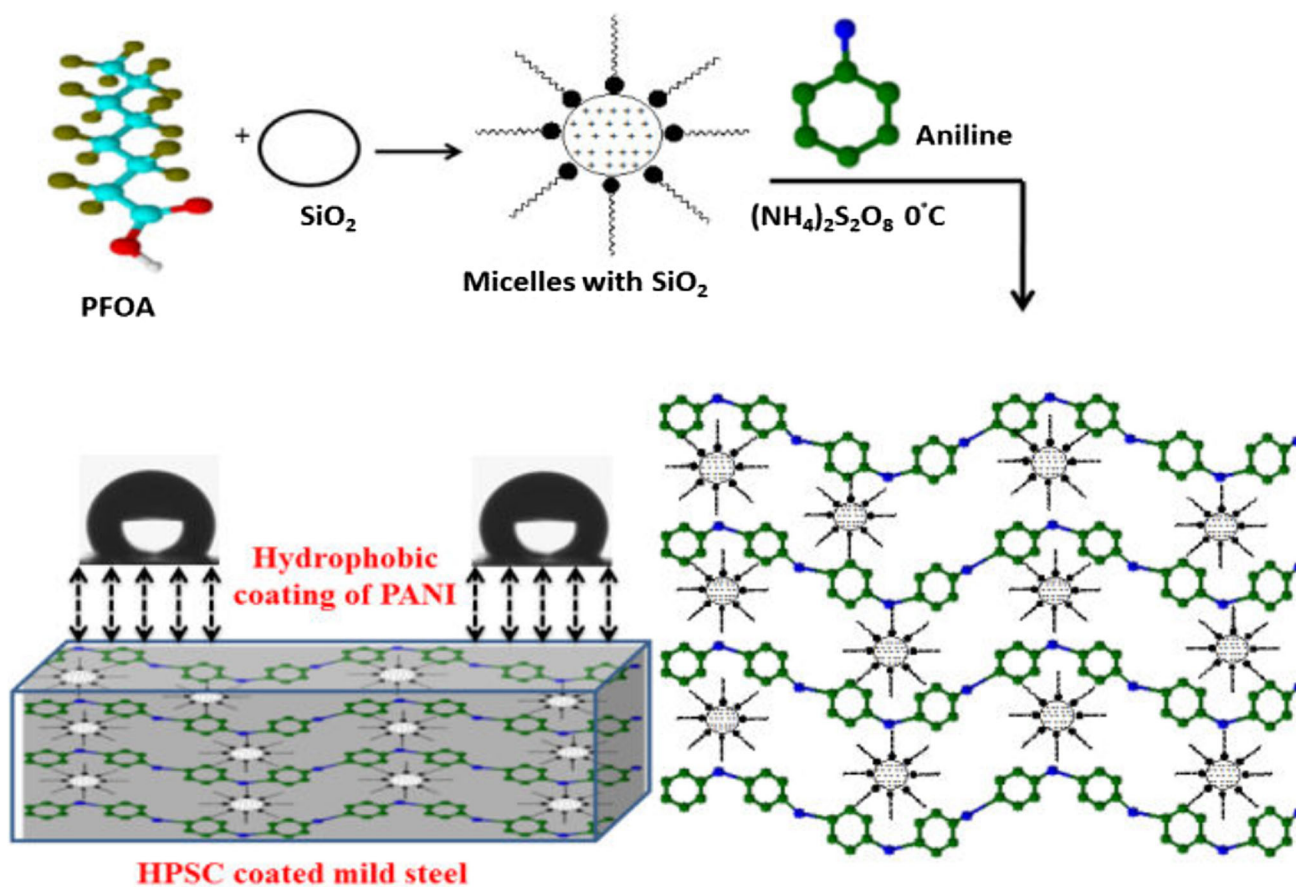


Fig. 6 Schematic representation of hydrophobic PANI-SiO₂ nanocomposites (Bhandari et al. 2012)

substrate. On the other hand, the entrapped SiO₂ nanoparticles into the PANI matrix decrease the PANI degradation in corrosive environments by strengthening PANI chains.

Certain interactions between poly(2,3-dimethylaniline), P(2,3-DMA), and SiO₂ nanoparticles seem to result in better thermal stability and electrochemical performance of the P(2,3-DMA)-SiO₂ nanocomposite in comparison with the P(2,3-DMA). It was reported that the P(2,3-DMA)-SiO₂ nanocomposite synthesized by in situ polymerization using SiO₂ nanoparticles was remarkably modified with respect to the poly(2,3-dimethylaniline) (P(2,3-DMA)) (Ma et al. 2014). Examining the anticorrosion properties of epoxy coatings containing simple P(2,3-DMA) and P(2,3-DMA)-SiO₂ nanocomposite showed that the P(2,3-DMA)-SiO₂ nanocomposite coating provided better protection to steel in 3.5 wt% NaCl than the simple P(2,3-DMA) coating. Improved anticorrosive properties of the P(2,3-DMA)-SiO₂ nanocomposite coating seem to be related to entrapped SiO₂ nanoparticles, which contribute to better barrier properties by reducing the transport of corrosive agents through the coating.

Hydrophobic polyaniline-boron nitride nanocomposites

Hierarchical PANI-boron nitride (BN) nanocomposites with a surface textured analogous to that of the Aloe-vera leaf were synthesized by in situ chemical polymerization of aniline in the presence of colloidal BN nanoparticles (ANI:BN = 37:1) and mixed with poly vinyl alcohol (PVA) to prepare coatings for the corrosion protection of mild steel (Sarkar et al. 2016). Sarkar et al. (2016) proposed that the 3D hierarchical evolution of PANI-BN nanocomposites is based on the morphological evolution of 1D nanofibers, as can be seen in Fig. 7. Aniline dimers and semidines result in the formation of trimers with phenazine moiety that constitute nucleates. Nucleates in acidic solution (pH < 2.5) are transformed to initiation centers for the following propagation of PANI chains and the growth of PANI nanofibers (Chiou and Epstein 2005a, b). The self-assembly of nucleates into 1D columnar structure is not favored in the presence of BN colloidal particles due to strong π - π interactions between the surface of BN and the

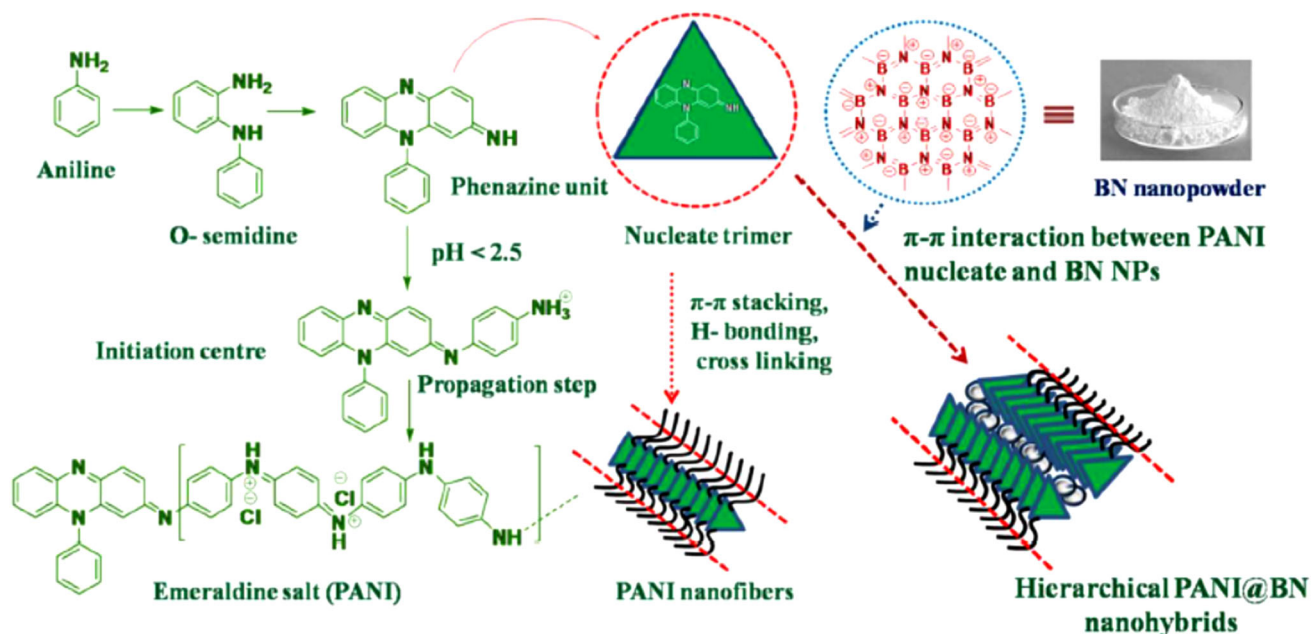


Fig. 7 Genesis of hierarchical PANI-BN nano hybrids. Reprinted with permission from (Sarkar et al. 2016) *Source:* Copyright 2016 American Chemical Society

nucleate that follows the hierarchical evolution of PANI chains with the core of the hierarchical tube filled up with self-assembled BN nanoparticles.

The corrosion resistance of mild steel samples painted with PANI-BN-PVA nanocomposites, PANI-PVA, and PVA coatings was investigated in 1 M HCl, 1 M H₂SO₄, and 3.5 wt% NaCl solutions by potentiodynamic polarization and EIS measurements. The PANI-BN-PVA coating exhibits enhanced anticorrosion efficiency as compared with PANI-PVA and PVA coatings. It was suggested that the ennobling of the open circuit potential and improved corrosion protection properties are associated with changes in the physicochemical properties of PANI, such as the crystallinity and hydrophobicity, due to the incorporation of BN nanoparticles into the core structure of PANI-BN nano hybrid material. The presence of the hierarchical PANI-BN nanocomposite improved the adhesion and mechanical properties of coatings by increasing the interactions between the PANI-BN and steel surface. Due to the rough surface and the improved hydrophobicity of PANI-BN-containing coatings, the transport of Cl⁻, H₂O, and O₂ is limited and the self-healing effect is enhanced. Eventually, there is a synergistic effect between PANI and nano BN particles that results in the suppression of steel electrodisolution improving concurrently the tendency for passivation.

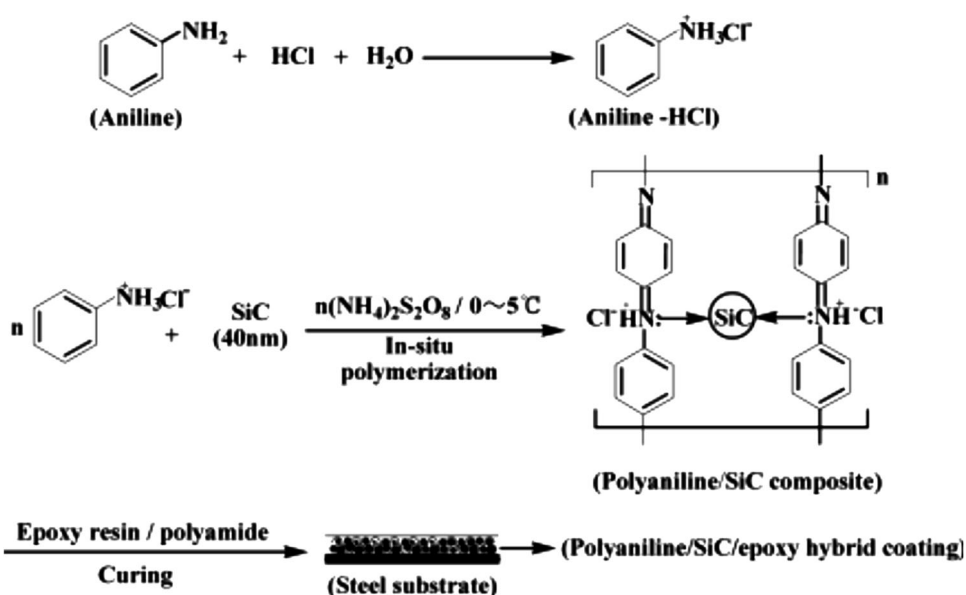
Polyaniline-SiC nanocomposites

Hu et al. (2016) reported recently that steel coupons coated with PANI-based coatings containing silicon carbide (SiC) nanoparticles exhibit enhanced corrosion resistance in 3.5

wt% NaCl compared with corresponding coupons coated with SiC-free PANI coatings (Hu et al. 2016). The PANI-SiC nanocomposites were synthesized by in situ chemical polymerization of aniline on the surface of SiC nanoparticles. As Fig. 8 shows, dispersion of the PANI-SiC material into epoxy (EP) resin and appropriate curing leads to the PANI-SiC/EP hybrid coatings. XRD analysis revealed that the crystalline structure of SiC nanoparticles is retained in the presence of PANI. Moreover, FTIR spectra indicated physicochemical interactions between PANI and SiC, likely through hydrogen bonds, since the characteristic peaks of PANI shift to lower wavenumbers.

Potentiodynamic polarization along with EIS measurements and immersion tests was carried out comparatively for uncoated steel and coated with PANI-SiC/EP, PANI/EP, and pure EP. The results indicated that the anticorrosion performance of PANI-SiC/EP hybrid coating was better than that of other coatings. The enhanced corrosion protection ability of the PANI-SiC/EP coating can be attributed to the formation of uniform passive layer on the steel surface and prevention of corrosion species to reach the substrate due to the barrier properties of SiC nanoparticles. SEM micrographs support the densification properties of the nanocomposite material, in concert with FTIR and UV spectra that indicated the existence of interactions between PANI and SiC. It was revealed that SiC nanoparticles are evenly dispersed in PANI matrix resulting in remarkable improvement of the compactness of the PANI structure. Similar enhanced corrosion protection properties were also recognized in the case of poly(o-toluidine)-SiC/EP nanocomposite coatings (Huang et al. 2015).

Fig. 8 Schematic representation of the preparation of PANI-SiC/EP hybrid coatings on steel surfaces (Hu et al. 2016)



Polyaniline-clay nanocomposites

Since first reports (Yeh et al. 2001, 2002) on the better anticorrosion performance of PANI-clay composites against the corrosion of cold-rolled steel in 5 wt% NaCl compared to that of conventional PANI coatings, many studies regarding the preparation and evaluation of corrosion protection properties of lamellar nanocomposites of PANI with various layered materials were reported (Akbarinezhad et al. 2011; Chang et al. 2007; Chang et al. 2006; De Riccardis and Martina 2014; Deshpande et al. 2014; Deshpande and Sazou 2015; Hosseini et al. 2011; Kalaivasan 2015; Kalaivasan and Shafi 2012; Navarchian et al. 2014).

Layered materials like smectite clays (e.g., montmorillonite, MMT) exhibit high aspect ratio, stiffness, and high in-plane strength. Two kinds of MMT are mostly used, namely hydrophilic montmorillonite (Na-MMT) and organophilic montmorillonite (O-MMT). Layered silicates such as MMT consist of negatively charged layers, which are stacked face to face forming crystallites, called also as tactoids, with a regular gap in between them (interlayer spacing or gallery). Depending on the synthesis route but primarily on the ANI:clay ratio, two types of structure can be obtained for PANI-clay nanocomposites: (i) intercalated nanocomposites where PANI chains are between the tactoids, resulting in regular repeated layers of clay and polymer, and (ii) exfoliated nanocomposites where clay crystallites are delaminated forming individual layers dispersed within the polymer.

Among synthetic approaches for preparing PANI-clay nanocomposite materials is the intercalation of anilinium salt inside the interlayer region where, after the addition of

the oxidizing agent, the ANI^+ -MMT as precursor drives in situ the chemical polymerization between the tactoids (Fig. 9) (Reena et al. 2009). Amphiphilic dopants like the dodecylbenzenesulfonic acid and camprorsulfonic acid are frequently used because they combine both hydrophilic and hydrophobic character by which can maximize the affinity between hydrophilic host (MMT) and hydrophobic guest (ANI) and, in addition, serve as a dopant for PANI.

Furthermore, PANI-clay nanocomposite materials have also been prepared by suspension and emulsion oxidative polymerization. By these routes, the polymerization may not necessarily occur inside the interlayer spacing (exfoliated nanocomposites). Though, several experimental observations support structurally restricted polymerization conditions for PANI in the presence of clay, the length of PANI chains and either the intra-chain or inter-chain PANI arrangements depend on the amount of clay or the PANI:clay ratio, the dopant and the polymerization route.

Chang et al. (2006) prepared nanocomposite materials comprising PANI and Na-MMT clay platelets through in situ chemical polymerization with APS as oxidizing agent and dodecylbenzenesulfonic acid (DBSA) as dopant and emulsifier/intercalating agent. The anticorrosion properties of the synthesized nanocomposite materials at low Na-MMT clay loading up to 3 wt% were investigated on cold-rolled steel (CRS) in 5 wt% NaCl in comparison with those of neat DBSA-doped PANI coatings. The coatings on CRS were prepared by dissolving first the DBSA-doped PANI and nanocomposite powder in NMP and the solutions were cast drop-wise on the CRS surfaces. Due to the relatively low content of Na-MMT clay, the PANI-Na-MMT nanocomposite exhibited a mixed nanostructure with individual layers along with multiple ones, up

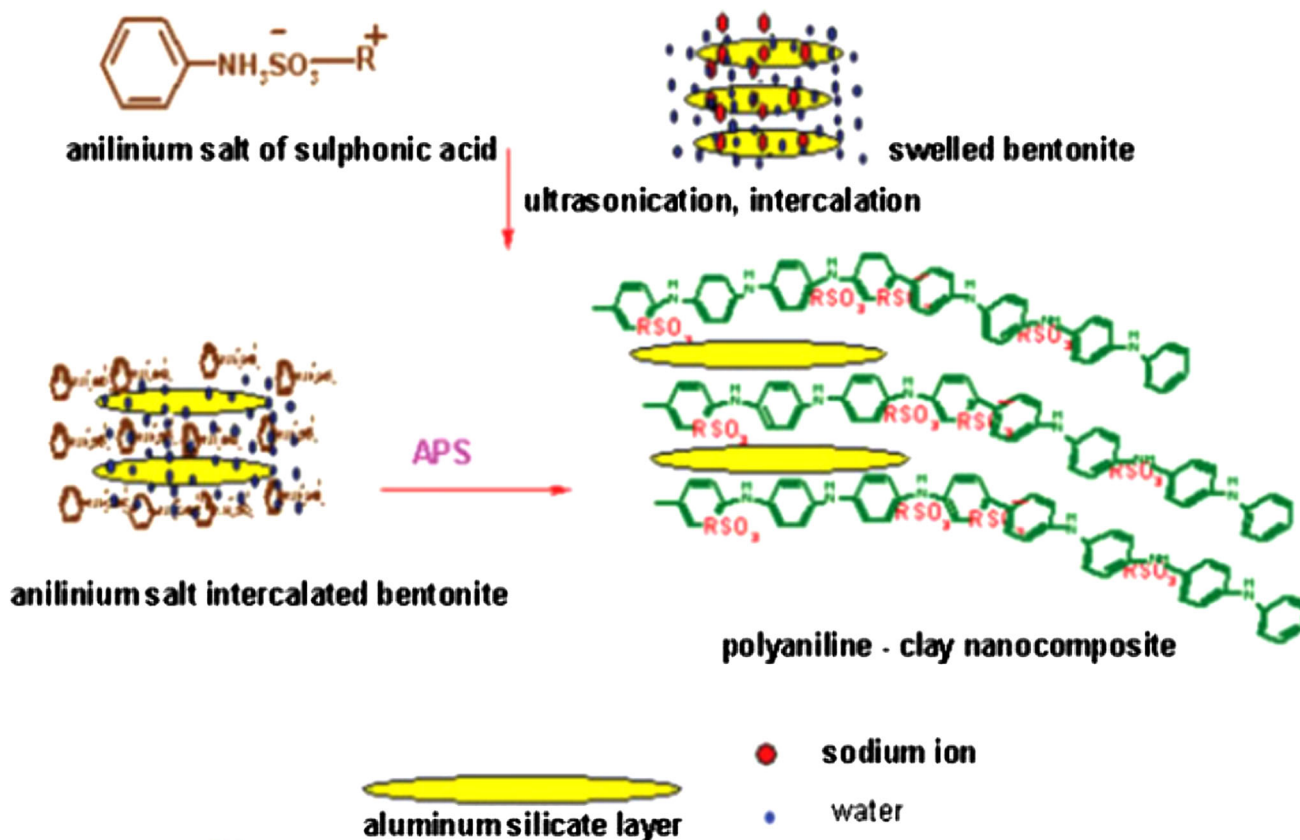


Fig. 9 Schematic representation of in situ oxidative polymerization of ANI between the interlayer region of clay where an amphiphilic sulfonic acid may serve concomitantly as intercalating precursor

ANI⁺-MMT and dopant for PANI Reprinted with permission from (Reena et al. 2009) Source: Copyright 2009 John Wiley and Sons

to four layer stacks, exfoliated into the PANI matrix. However, despite the low clay amount, the electrical conductivity of PANI-Na-MMT nanocomposite was found to be lower than that of the DBSA-doped PANI. This behavior was rationalized by the decreasing molecular weight of PANI existing in the nanocomposite, which evaluated by gel permeation chromatography was found to be remarkably lower than that of the neat PANI. This explanation was further supported by the higher electrical conductivity found for the nanocomposite of PANI with organophilic, O-MMT clay (PANI-O-MMT) in the presence of the same amount of clay, which exhibited a higher molecular weight (Chang et al. 2006). The electrical conductivity is associated with the continuous conductive network through the composite, which seems to be limited in these nanocomposites implying perhaps a reduction of radical cation segments in PANI chains due to the confinement of the polymeric chains (Do Nascimento et al. 2006).

On the basis of potentiodynamic polarization and EIS measurements, PANI-Na-MMT nanocomposite coatings were found to be superior in corrosion protection of CRS in 5 wt% NaCl than the DBSA-doped PANI due to the

combination of the redox catalytic property of PANI and the molecular barrier effect of MMT clay platelets dispersed in nanocomposites. The enhancement of the molecular barrier effect of PANI-Na-MMT nanocomposite coatings might be due to the dispersed silicate monolayer of MMT clay in the PANI matrix resulting in a lower permeability of H₂O and O₂ through the nanocomposite and in lengthening of their diffusion pathways. Moreover, the PANI-Na-MMT nanocomposite coating containing 3 wt% Na-MMT clay exhibited better corrosion protection effect on CRS than the PANI-O-MMT nanocomposite coating with the same clay loading (3 wt%) (Chang et al. 2006).

In another study, Chang et al. (2007) investigated comparatively the anticorrosive properties of PANI-Na-MMT nanocomposite (at 1 wt% Na-MMT clay loading) and DBSA-doped PANI coatings on CRS at different operational temperatures and found that the corrosion potential of uncoated, DBSA-doped PANI and PANI-Na-MMT-coated CRS all shifted to lower values indicating more severe corrosion in 5 wt% NaCl upon increasing the operational temperature from 30 to 50 °C. However, even under relatively high temperatures the DBSA-doped PANI

and PANI-Na-MMT nanocomposite coatings protect effectively CRS coupons. The decrease of the polarization resistance in the case of PANI-Na-MMT nanocomposite coatings was lesser than for the uncoated and PANI-coated CRS (Chang et al. 2007). These findings might be associated with the increase in the electrical conductivity of PANI-Na-MMT nanocomposites caused by increasing the operational temperature within the same range, though the effect of the operational temperature was not provided on the as prepared DBSA-doped PANI but for PANI doped with inorganic acids. In the same study, authors studied the temperature effect on PANI and PANI-Na-MMT nanocomposite doped with HCl, HNO₃, and H₂SO₄. It was shown that the effect of the type and size of dopant on the electrical conductivity of the PANI-Na-MMT nanocomposite is similar with that of the neat PANI though electrical conductivity values are lower than those for PANI, by almost one order of magnitude. The electrical conductivity followed the order HCl > HNO₃ > H₂SO₄ for both PANI and PANI-Na-MMT nanocomposite due perhaps to the smaller size of Cl⁻ relatively to the size of other dopant anions (Chang et al. 2007).

An enhancement of anticorrosion properties was also observed in the case of nanocomposite coatings comprising poly(o-methoxyaniline) (PMA) and Na-MMT clay (Yeh et al. 2007). DBSA-doped PMA and PMA-Na-MMT nanocomposite along with corresponding coatings were prepared through the same chemical polymerization routes and preparation methods used in above-mentioned studies (Chang et al. 2006, 2007). PMA-Na-MMT nanocomposite coatings at low Na-MMT clay loading (up to 5 wt%) exhibited better corrosion protection efficiency for the CRS in 5 wt% NaCl than the neat DBSA-doped PMA. This effect was assigned to the combination of the redox catalytic property of PMA with the barrier effect of MMT clay platelets against the transport of O₂ and H₂O through the coating, as in the case of PANI-based analogous nanocomposite coatings. Likewise, the electrical conductivity of the PMA-Na-MMT nanocomposite was found to be lower than that of the DBSA-doped PMA implying perhaps a decreased conjugated chain length of the PMA within the Na-MMT clay. This observation seems consistent with the blue shift of the excitation absorption peak in UV-Vis spectra for nanocomposites and the lower molecular weight found for the PMA existing in nanocomposites.

Olad and Rashidzadeh (2008) prepared nanocomposites of PANI with organophilic montmorillonite (O-MMT) and hydrophilic montmorillonite (Na-MMT) by in situ chemical oxidative polymerization of ANI in 1.5 M HCl using as oxidant agent the APS. In this study, the role of hydrophilic and organophilic MMT on the anticorrosion effectiveness of PANI-based nanocomposite coatings is examined comparatively. Cyclic voltammetric measurements of nanocomposites

on Au have shown that both PANI-Na-MMT and PANI-O-MMT (with 5 wt% MMT content) exhibit reversible electrochemical redox behavior with slightly higher anodic/cathodic currents in the case of the latter nanocomposite. In agreement, with this behavior, the PANI-O-MMT exhibited higher (29.4%) electrical conductivity than the PANI-Na-MMT nanocomposite (5.8%) and the neat PANI. This result is consistent with the trend reported by Chang et al. (2006).

Coatings of PANI-Na-MMT and PANI-O-MMT nanocomposites and neat PANI were prepared by the casting method using NMP as solvent. The corrosion protection performance of three coatings was investigated comparatively by potentiodynamic polarization measurements for iron samples in 3.5 wt% NaCl and 1 M H₂SO₄. On the basis of corrosion potential, E_{corr} and corrosion current, I_{corr} , Olad and Rashidzadeh (2008) found that both nanocomposites might offer better corrosion protection than neat PANI only in 3.5 wt% NaCl. In contrast, in 1 M H₂SO₄ both the E_{corr} and I_{corr} for nanocomposites shift to higher values with respect to corresponding values evaluated for PANI. It should be noted that these findings did not match neither with corrosion rates evaluated by authors, in the same work, nor with the final conclusion of the study (Olad and Rashidzadeh 2008). Both E_{corr} and I_{corr} values were lower for PANI-O-MMT than for PANI-Na-MMT nanocomposite coatings in both 3.5 wt% NaCl and 1 M H₂SO₄. This trend is different from that reported by Chang et al. (2006) in 5 wt% NaCl but in agreement with that observed by other authors (Navarchian et al. 2014).

Differences observed in various studies are perhaps originated from different preparation methods used. In fact, Navarchian et al. (2014) used PANI and PANI-MMT nanocomposite as pigments into epoxy paint, while Olad and Rashidzadeh (2008) and Chang et al. (2006) applied PANI and PANI-MMT nanocomposite as primers using the same casting method. On the other hand, for the synthesis of PANI-MMT nanocomposites, in situ emulsion polymerization in the presence of DBSA was used by Chang et al. (2006) and suspension polymerization in the presence of HCl by Olad and Rashidzadeh (2008) and Navarchian et al. (2014). Therefore, differences may be also originated from different polymerization routes and dopant anions used as both factors are expected to influence the structure and physicochemical properties of PANI-based coatings.

The anticorrosive properties of PANI-Na-MMT- and PANI-O-MMT-based pigments along with those of the PANI pigment were studied comparatively for steel substrates in 3.5 wt% NaCl aiming to examine the effect of clay addition and the type of clay cation, including Na⁺ in natural clay (Na-MMT) and alkyl ammonium ions in organo-modified montmorillonite (O-MMT) (Navarchian et al. 2014). The results from several corrosion tests, including potentiodynamic polarization, EIS, and weight

loss measurements, agree that the addition of PANI-O-MMT nanocomposite into epoxy paint promotes corrosion protection of steel more effectively than PANI-Na-MMT nanocomposite and neat PANI do. This trend was rationalized by considering the higher adhesion strength of the PANI-O-MMT nanocomposite into epoxy paint on steel, which was remained almost constant during immersion for 30 days in the NaCl solution compared to pigments containing PANI-Na-MMT and PANI (Navarchian et al. 2014). The higher adhesion strength may be originated from the hydrophobic nature of O-MMT compared to Na-MMT that restricts water uptake and transport of electrolyte solution through the coating (Bagherzadeh and Mousavinejad 2012).

Akbarinezhad et al. (2011) synthesized PANI-based clay nanocomposite by in situ suspension oxidative polymerization of ANI with APS in the presence of Cloisite 30B nanoclay, which is an organophilic MMT (O-MMT). SEM images revealed that the PANI-O-MMT nanocomposite exhibits tightly packed particles of nanoclay and PANI nanoparticles with size ranged from 70 to 150 nm. It was found that the electrical conductivity of PANI-O-MMT is almost one order of magnitude higher than that of pristine PANI ($\sigma = 6.3 \times 10^{-5} \text{ S cm}^{-1}$). Though this result is opposite compared to that reported in above studies, is in agreement with observations reported by Reena et al. (2009) where experimental data support the strong influence of the PANI:clay ratio and dopant anion used on the electrical conductivity and structure of PANI-clay nanocomposites. At relatively high concentrations of PANI, the insulative clay may interrupt the 3-D organization of PANI chains and lead to expanded conformation of PANI chains in a confined environment where charge delocalization is promoted resulting in a higher electrical conductivity for the PANI-MMT composite than for PANI.

The effect of the addition of PANI-O-MMT on the anticorrosion properties of ethyl silicate zinc-rich primer (ZRP) was examined by modifying the primer with PANI-O-MMT. The anticorrosion performance of the PANI-O-MMT-modified ZRP was investigated in comparison with that of the unmodified primer on carbon steel panels in 3.5 wt% NaCl for a period of 120 days. Open circuit potential and EIS measurements have shown that the open circuit potential and polarization resistance were higher for the PANI-O-MMT-modified ZRP coating than for the unmodified ZRP after 120 days of immersion. The open circuit potential for both coatings remained lower than $-0.8 V_{\text{SCE}}$ during the period of 120 days indicating the active contribution of zinc particles. The improved corrosion protection of the PANI-O-MMT-modified ZRP was attributed to the electrochemical active contribution of PANI-O-MMT nanocomposite through the promotion of

the metal substrate passivation and barrier effects (Akbarinezhad et al. 2011).

Kalaivasan and Shafi (2012) suggested the synthesis of PANI-Na-MMT nanocomposites by employing a solvent-free mechanochemical method, which involves the direct intercalation of anilinium chloride into Na-MMT layers and in situ polymerization within interlayer region. After grinding Na-MMT with anilinium chloride, the APS was added and the mixture was ground also mechanochemically (Kalaivasan and Shafi 2012). It was shown that the HCl-doped PANI-MMT nanocomposite coatings on C45 demonstrated a better anticorrosion performance in 3.5 wt% NaCl over that of conventionally synthesized PANI-Na-MMT nanocomposite coatings (Kalaivasan 2015).

Clinoptilolite (Clino), a widely distributed zeolite mineral in nature, was also found to enhance the anticorrosive properties of PANI when PANI-Clino nanocomposite was used in the form of a coating for iron protection (Olad and Naseri 2010). Clinoptilolite has a two-dimensional layer-like structure in which $(\text{Si,Al})\text{O}_4$ tetrahedral are connected via oxygen atoms in layers. The PANI-Clino nanocomposite was prepared using natural clinoptilolite by chemical oxidative polymerization of anilinium cations facilitating the replacement of protons in acidic clinoptilolite. PANI-Clino nanocomposites with 1, 3, and 5% w/w of clinoptilolite content were examined as anticorrosive coatings (20 μm in thickness) on iron surfaces in different corrosive media, namely 1 M H_2SO_4 , 1 M HCl, and 3.5 wt% NaCl. Corrosion tests in acid environments demonstrated that the PANI-Clino nanocomposite has better protection effect than the neat PANI coating. The anticorrosive properties of nanocomposite proved to depend on both the clinoptilolite content and the corrosive medium. In particular, the PANI-Clino nanocomposite coating with 3% (w/w) clinoptilolite exhibited the highest protective efficiency for iron in all the above-mentioned corrosive media. In conclusion, appropriate encapsulation of PANI in clinoptilolite channels and dispersion of clinoptilolite layers into the PANI matrix stimulate the anticorrosive performance of PANI-Clino nanocomposite coating preventing the diffusion pathway of corrosive agents towards the iron surface (Olad and Naseri 2010).

Layered double hydroxides (LDHs) constitute another type of clay materials used in the preparation of polymer nanocomposites. Hu et al. (2014) prepared PANI-LDH-based nanocomposites by chemical grafting of the PANI onto LDH. Decavanadate anion ($\text{V}_{10}\text{O}_{28}^{6-}$) with anticorrosion ability was intercalated into Zn-Al-NO_3 -LDH via an anion-exchange reaction leading to the D-LDH. The D-LDH was treated with APS to form a bonding layer on its surface. The PANI-clay composite was synthesized by in situ oxidative polymerization on the APS-treated D-LDH surface (AD-LDH) and is designated as PANI-AD-

LDH. The corrosion protection effectiveness of the PANI-AD-LDH nanocomposite was examined in epoxy pigments applied on mild steel. The PANI-AD-LDH nanocomposite coating demonstrated a higher anticorrosion effect against the corrosion of mild steel in 3.5 wt% NaCl than the individual components D-LDH and PANI. The higher corrosion protection ability of coatings containing PANI-AD-LDH nanocomposite has been attributed to: (i) the increase of the length of diffusion pathways for O₂ and H₂O and decrease of the permeability of the coating, (ii) the redox properties of PANI by which the formation of the passive oxide film on steel is stimulated and (iii) the presence of inhibiting anions (V₁₀O₂₈⁶⁻), which, if a defect is generated, may be released by the reduction of the EB form of PANI to retard the corrosion of steel (Hu et al. 2014).

Polyaniline-graphene nanocomposites

The lower density and higher aspect ratio of conductive graphene relative to nonconductive clay platelets induced a great deal of interest in utilizing graphene for the preparation of nanocomposite materials in designated applications, such as energy storage devices (Li et al. 2013a) and innovative gas (e.g., O₂ and H₂O) barrier polymer composite films (Compton et al. 2010). Polymer-graphene composites being good O₂ and H₂O gas barriers initiated also the interest for their application as anticorrosive coatings (Singh et al. 2013a, b). Within this context, novel PANI-graphene composite anticorrosion coatings were obtained through exfoliating and functionalizing by a direct electrophilic substitution reaction with 4-aminobenzoic (ABA) in polyphosphoric acid (PPA)/P₂O₅ (Fig. 10). This method was developed for graphene functionalization (Choi et al. 2010) and applied widely for several carbon-based materials (e.g., carbon nanotubes, diamond, and fullerenes). The chemical oxidative polymerization of ANI with different amounts of 4-aminobenzoyl group-functionalized graphene-like (ABF-G) sheets was carried out in 1.0 M HCl solution of the oxidant APS to provide PANI-graphene composites (PAGCs) (Chang et al. 2012). The graphene was found to be well dispersed into the PANI matrix. The electrical conductivity of the PANI-graphene composites with 0.5 wt% ABF-G loading was one order of magnitude higher than that of PANI. As conductive filler the graphene does not cause a decrease but on the contrary leads to an increase of the electrical conductivity of PANI. This is not always the case for PANI-clay nanocomposite materials as clay is an insulator.

PANI-graphene composite was dispersed in NMP and coatings were prepared by the casting method onto the steel substrate. The anticorrosive properties of PANI-graphene

composites in the form of coatings on steel were investigated in 3.5 wt% NaCl (Chang et al. 2012). On the basis of comparative results obtained for PANI-graphene and PANI-clay nanocomposite coatings was concluded that well-dispersed graphene in the PANI matrix, with a relatively high aspect ratio compared with clay, enhances the impermeability of the coating to gas molecules like O₂ and H₂O. The enhancement of the coating impermeability to these molecules along with other properties makes PANI-graphene coatings perhaps more suitable materials in anticorrosion applications than PANI-clay nanocomposite coatings.

Polyaniline-carbon nanotube composites

Composite materials based on the coupling of carbon nanotubes (CNTs) with PANI and its derivatives constitute multifunctional materials, which retain properties of individual components via a synergistic effect (Baibarac and Gomez-Romero 2006). CNTs can be classified into two main categories: single-walled carbon nanotubes (SWNTs) and multi-walled carbon nanotubes (MWNTs). The former results from a single graphene sheet, whereas the latter from additional graphene sheets wrapped around the SWNT core. In PANI-CNTs nanocomposites, either the polymer functionalizes CNTs or the PANI is doped with CNTs and charge transfer takes place between the two components via the formation of donor–acceptor complexes (Fig. 11).

PANI-CNTs nanocomposites have a great potential in many applications including anticorrosion technology. Electrochemical deposition of neat PANI and PANI containing two different types of CNTs was carried out on stainless steel (AISI 304) substrates. The results suggested that PANI was synthesized electrochemically onto the CNTs acting as backbone due to a donor–acceptor effect created between PANI and CNTs (Fig. 11). Thus, the presence of CNTs in the PANI matrix leads to an increase of the amount of PANI electrodeposited on the substrate. The PANI-CNTs nanocomposite films displayed an enhanced anticorrosion performance for AISI 304 in sulfuric acid solutions due to the improved blocking effect of the composite material regarding transport of corrosion products as compared with that of PANI films. Furthermore, comparing between two kinds of CNTs suggested that the blocking property is better for CNTs of smaller diameter and higher length (Martina et al. 2011).

Deshpande et al. (2013) formulated PANI-MWNTs nanocomposite paint coating. The corrosion rate was shown to be 5.2 times lower than that of unpainted low carbon steel samples (Deshpande et al. 2013). The good corrosion protection performance of the PANI-MWNTs nanocomposite paint coating might be due to the larger surface area and the higher conductivity of the PANI-

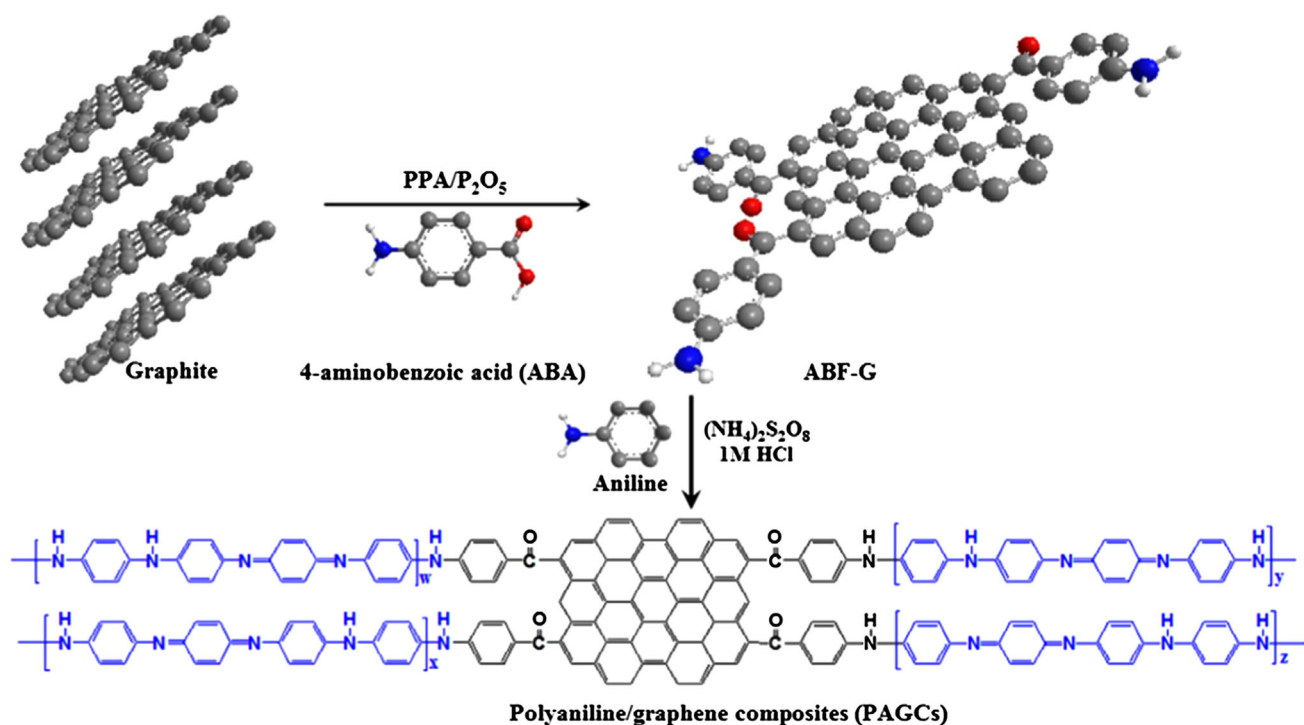


Fig. 10 Schematic representation of the preparation of PANI-graphene composites. Reprinted with permission from (Chang et al. 2012) *Source:* Copyright 2012 Elsevier

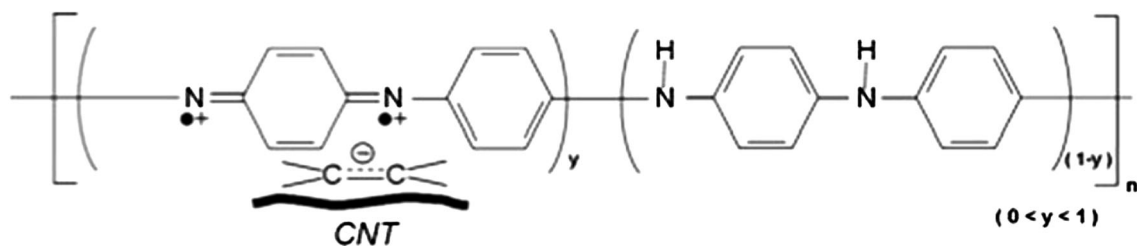


Fig. 11 Illustration of the interaction between PANI and CNTs (Martina et al. 2011) *Source:* With permission of Springer

MWNTs nanocomposite relatively with the neat PANI (Konyushenko et al. 2006). The surface modification of MWCNTs with PANI and the electronic interaction between the two ingredients bring functional groups on the PANI surface that may affect the interaction with the polymer matrix constituting the paint.

The physicochemical properties of PANI-MWNTs nanocomposites can be tuned by functionalization with carboxylic acid and amino groups PANI. Functionalization can be carried out by appropriate treatment of MWCNTs leading to carboxylated and amino CNTs (f-CNTs), from which PANI-f-CNTs nanocomposite coatings can be prepared by in situ chemical oxidative polymerization of ANI (Kumar and Gasem 2015a) or electrochemical polymerization (Kumar and Gasem 2015b) on mild steel (MS) surface from an aqueous oxalic acid solution containing 0.1 M ANI and 0.01 M sodium

dodecyl sulfate. In the latter case, the PANI-f-CNTs nanocomposite coating was directly deposited on the metal substrate whereas in the former case the dipping method was used. The resulted PANI-f-CNTs nanocomposite coatings displayed uniform dispersion of f-CNTs into the PANI matrix, improved mechanical properties and hydrophobicity dependent on the f-CNTs content. Upon increasing the f-CNT content both the hardness and the surface hydrophobic character of the coating were increased. On the basis of electrochemical corrosion tests, it was shown that the inclusion of CNTs into the PANI coating can lead to a notable increase in the corrosion resistance of MS in 3.5 wt% NaCl solution. The best protective performance was found for PANI-f-CNTs nanocomposites with good dispersion of the functionalized CNTs into the PANI matrix and strong interaction between PANI and CNTs (Kumar and Gasem 2015a).

Design care

There is evidence that nanoparticles (<100 nm) such as SiO₂ and TiO₂ can be hazardous to humans and can display ecotoxicity. Therefore, in the design of nanocomposites with such nanoparticles, hazard reduction extending to the full nanocomposite life cycle would seem an issue of concern. Possibilities for hazard reduction comprise: modifications of nanoparticle surface, crystal structure, morphology, composition, well fixation of nanoparticles in nanocomposites, including persistent suppression of oxidative damage to polymers by nanoparticles and applicable strategies leading to the liberation of fairly large particles (Reijnders 2009). Given further advances in tailoring nano-scale architectures of PANI and SiO₂ or TiO₂ particles toward enhanced activity and durability in anti-corrosion technology and other applications, further progress in hazard reduction approaches is expected alongside novel multifunctional materials.

Conclusions

Encapsulation of nanofillers such as metal and metal oxide particles, nanoclays, graphene and carbon nanotubes in PANI chain results in novel nanocomposite materials,

suitable for the development of self-healing functional coatings exploited in metal anticorrosion protection. PANI nanocomposites combining the qualities of conducting PANI and inorganic nanoparticles display better mechanical, physical, and chemical properties than the parent PANI and can function as effective pigments in anticorrosive coatings for steel. The improved protective performance of PANI-based nanocomposite coatings is mostly associated with synergistic effects by which anodic or cathodic protection mechanisms of PANI are enhanced prolonging the service life of coatings. Control of the physico-electrochemical properties of PANI nanocomposites through appropriate selection of synthesis parameters and component materials will be necessary for the development of protective PANI-based nanocomposite coatings with pre-determined properties to meet efficiently and persistently operational conditions of metals in specific corrosive environments.

Appendix

See Tables 2, 3, 4.

Table 2 Nanocomposites of PANI with metal and metal oxide nanoparticles

Nanocomposite	Coating composition/substrate/corrosive medium	Synthesis method	Coating characterization	Salient features	References
PANI–Zn	PANI–Zn in NMP/Fe/0.1 M HCl 0.1 M H ₂ SO ₄ 3.5 wt% NaCl	In situ chemical polymerization in presence of APS, HCl	FTIR, AFM, OCP monitoring, four probe technique, potentiodynamic polarization, CV	Increasing conductivity with Zn content up to 5 wt% Zn nanoparticle size ~ 80 nm Synergistic effect	Olad and Rasouli (2010)
PANI–Zn	PANI–Zn in NMP/Fe/0.1 M HCl	Solution mixing method	FTIR, XRD, SEM, four probe technique, EIS, OCP monitoring, potentiodynamic polarization	Best anticorrosion effect at 4 wt% Zn loading Increased tortuosity of the diffusion path of corrosive species	Olad et al. (2011)
PANI–Zn	PANI–Zn -epoxy/Fe/0.1 M HCl	Solution mixing method	FTIR, XRD, SEM, potentiodynamic polarization, OCP monitoring	Improved mechanical and barrier properties Best corrosion protection effect at 4 wt% Zn and 3–7 wt% epoxy	Olad et al. (2012)

Table 2 Nanocomposites of PANI with metal and metal oxide nanoparticles

Nanocomposite	Coating composition/substrate/corrosive medium	Synthesis method	Coating characterization	Salient features	References
PANI–ZnO	DBSA-PANI–ZnO- PVAc/steel/ 3.5 wt% NaCl	Solution mixing method	XRD, SEM, cyclic voltammetry, potentiodynamic polarization, OCP monitoring	Synergistic effect results in an enhanced barrier effect	Patil and Radhakrishnan (2006)
PANI–ZnO	PANI–ZnO-epoxy/steel/3.5 wt% NaCl	In situ emulsion polymerization in the presence of APS, CSA	FTIR, XRD, SEM, TEM, TGA, four probe technique, adhesion strength, OCP monitoring, EIS	Release of DBSA when PANI is reduced at coating defects Best corrosion protection effect at 2 wt% ZnO loading	Mostafaei and Nasirpour (2014)
PANI–ZnO	PANI–ZnO- epoxy/steel/3.5 wt% NaCl	In situ emulsion polymerization in the presence of APS, CSA	FTIR, XRD, SEM, TEM, TGA four probe technique, OCP monitoring, EIS	Flaky- shaped structure Increasing the temperature from 25 °C to 65 °C the coating resistance remains sufficiently high	Mostafaei and Nasirpour (2013, 2014)
PANI–ZnO	PANI–PVC–ZnO/Fe/3.5 wt% NaCl	In situ chemical polymerization in the presence of APS, HCl	FTIR, XRD, SEM, TEM, four probe technique, potentiodynamic polarization, OCP monitoring	ZnO particles expand barrier and electrochemical properties of PANI PVC strengthens barrier ability	Olad and Nosrati (2013)
PANI–ZnO	PANI–ZnO in NMP/steel and Al/ 0.1 M HCl 1 M NaCl	In situ chemical polymerization in the presence of APS, HCl	SEM, cyclic voltammetry, potentiodynamic polarization, EIS	Increased adhesion strength on steel Anodic protection mechanism	Alvi et al. (2015)
PoPDA–ZnO	PoPDA–ZnO/AISI304 stainless steel/3.5 wt% NaCl	Potentiostatic deposition	FTIR, SEM, OCP monitoring, potentiodynamic polarization, EIS	ZnO nanoparticles catalyze the reduction of O ₂ on PoPDA Increased ability of PoPDA to plug defects initiating oxide formation	Ganash (2014)
PANI–ZnO poly(XY)-ZnO poly(PA)-ZnO poly(ANI-co-PA-co-XY)-ZnO	Nanocomposites in epoxy resin/ mild steel/0.1 M HCl	In situ chemical polymerization	FTIR, XRD, SEM, OCP monitoring, weight loss measurements, potentiodynamic polarization, EIS	Terpolymer nanocomposite coating superior in corrosion protection during prolonging immersion Strong interactions between terpolymer chain and ZnO particles	Alam et al. (2016)
PANI–TiO ₂	PANI–TiO ₂ /stainless steel/3.5 wt% NaCl	In situ chemical polymerization in presence of APS, HCl	SEM, OCP monitoring, potentiodynamic polarization, weight loss measurements, EIS	p-n junction effect Enhanced anticorrosion property due to a synergistic effect	Radhakrishnan et al. (2009)
PANI–TiO ₂	PANI–TiO ₂ -epoxy/carbon steel/ 3.5wt%NaCl 5 wt% HCl 5wt% NaOH	In situ emulsion polymerization	FTIR, XRD, SEM, TEM, OCP monitoring, weight loss measurements, EIS	Enhanced barrier property and oxide formation ability p–n junction effect	Mahulikar et al. (2011)

Table 2 continued

Nanocomposite	Coating composition/substrate/corrosive medium	Synthesis method	Coating characterization	Salient features	References
PANI–TiO ₂	Oxalic acid–PANI–TiO ₂ /steel/1 wt% NaCl	Cyclic voltammetry from oxalic acid + ANI solution	Cyclic voltammetry, FTIR, XPS	Improved, stable electroactivity Strong interactions between PANI chains and TiO ₂ nanoparticles	Karpakam et al. (2011)
PDMA–TiO ₂	PANI–TiO ₂ –epoxy/steel/3.5 wt% NaCl	In situ chemical polymerization in presence of APS, H ₃ PO ₄	FTIR, XRD, SEM, OCP monitoring, EIS	TiO ₂ nanoparticles enhanced the barrier effect and the liberation of dopant/inhibitor when PDMA was reduced	Li et al. (2013a, b)
PANI–TiO ₂	PANI–TiO ₂ /A304 stainless steel/1 M H ₂ SO ₄	Cyclic voltammetry from LiClO ₄ –H ₂ SO ₄ +ANI solution	Cyclic voltammetry, potentiodynamic polarization, EIS, SEM	Decrease of PANI degradation and porosity due to the presence of TiO ₂ particles	Abaci and Nessark (2015)
POT–ZrO ₂	POT–ZrO ₂ /mild steel/3 wt% NaCl	Cyclic voltammetry from tartrate + ANI solution	Cyclic voltammetry, potentiodynamic polarization, EIS, SEM	Uniform and smooth morphology Low porosity Prevention of chloride transport	Chaudhari et al. (2007)
POT–CdO	POT–CdO/mild steel/3 wt% NaCl	Cyclic voltammetry from tartrate solutions of o-toluidine	Cyclic voltammetry, UV–Vis, FTIR, XRD, SEM, EIS, potentiodynamic polarization	Low porosity Reduced corrosion rate Increased corrosion resistance	Chaudhari et al. (2010)
PANI–ferrite	PANI–ferrite–alkyd/steel/3.5 wt% NaCl 5 wt% HCl 5 wt% NaOH	In situ chemical polymerization and dispersion into alkyd	UV–Vis, SEM, weight loss measurements	Dense, nonporous continuous network-type morphology High resistance to corrosive ions	Alam et al. (2008)
PANI–ferrite	PANI–ferrite–alkyd/steel/3.5 wt% NaCl 3.5 wt% HCl 3.5 wt% NaOH	In situ chemical polymerization and dispersion into alkyd	Potentiodynamic polarization	Low corrosion rate Good corrosion protection efficiency	Alam et al. (2010)
PANI–Fe ₂ O ₃ .NiO	PANI–Fe ₂ O ₃ .NiO in polyurethane matrix/steel/3 wt% NaCl	Precipitation–oxidation method	XRD, magnetization, electric conductivity, SEM, EIS	Magnetic and electric properties depend on Fe ₂ O ₃ .NiO content	Nghia and Tung (2009)
PANI–SiO ₂	PANI–SiO ₂ /mild steel (powder coating method)/3.5 wt% NaCl	In situ chemical polymerization of ANI in APS, 0.2 M H ₃ PO ₄ /0.2 M PFOA	FTIR, UV–vis TGA, SEM, weight loss measurements, chronoamperometry, potentiodynamic polarization,	Hydrophobic character Reinforcement of PANI chains High resistance to transport of chlorides	Bhandari et al. (2012)
P(2,3-DMA)–SiO ₂	P(2,3-DMA)–SiO ₂ /steel/3.5 wt% NaCl	In situ chemical polymerization in the presence of APS, HCl	FTIR, TGA, cyclic voltammetry, EIS, OCP monitoring potentiodynamic polarization	Improved barrier properties Better thermal stability Delay in transport of corrosive agents through coating	Ma et al. (2014)

Table 3 Nanocomposites of PANI with clay materials

Nanocomposite	Coating composition/substrate/corrosive medium	Synthesis method	Coating characterization	Salient features	References
PANI-O-MMT	PANI-O-MMT in NMP (1 wt%)/CRS/5 wt% NaCl	In situ polymerization of ANI in the presence of APS, HCl (0.25, 0.5, 0.75 wt% O-MMT)	FTIR, XRD, TEM, TGA, GPC, gas permeability, differential scanning calorimetry, dynamic mechanical analysis, potentiodynamic polarization	Reduction in O ₂ permeability Decrease of PANI molecular weight, mechanical strength and thermal decomposition temperature Better anticorrosion performance	Yeh et al. (2001)
PEA-O-MMT	PEA-O-MMT in NMP (0.75 wt%)/CRS/5 wt% NaCl	In situ polymerization in the presence of APS, HCl (0.5, 1, 3, 5 wt% O-MMT)	FTIR, XRD, TEM, TGA, GPC, gas permeability analyzer, four-probe technique, UV-vis, EIS, potentiodynamic polarization	Enhancement in gas impermeability up to 3 wt% MMT Decrease of PEA molecular weight and electrical conductivity	Yeh et al. (2002)
PANI-Na-MMT PANI-O-MMT	DBSA-doped PANI-MMT in NMP (1 wt%)/CRS/5 wt% NaCl	In situ emulsion polymerization in the presence of APS, DBSA (0.5, 1, 3 wt% MMT)	FTIR, XRD, TEM, UV-Vis, gas permeability analyzer, four-probe technique, potentiodynamic polarization, EIS	Decreased conductivity Enhancement in gas impermeability Higher conductivity, and anticorrosion performance for PANI-O-MMT	Chang et al. (2006)
PANI-Na-MMT	DBSA-doped PANI-Na-MMT in NMP (1 wt%)/CRS/5 wt% NaCl	In situ emulsion polymerization of ANI in the presence of APS, DBSA (1 wt% MMT)	FTIR, XRD, TEM, UV-Vis, gas permeability analyzer, four-probe technique, potentiodynamic polarization, EIS	Lesser decrease of the anticorrosion property of PANI-Na-MMT with operational temperature (30–50 °C) than that of PANI	Chang et al. (2007)
PMA-Na-MMT	DBSA-doped PMA-Na-MMT in NMP (1 wt%)/CRS/5 wt% NaCl	In situ emulsion polymerization in the presence of APS, DBSA (1, 3, 5 wt% MMT)	FTIR, XRD, SEM, TGA, UV-Vis, gas permeability analyzer, four probe technique, potentiodynamic polarization, EIS	Enhancement in the barrier effect against permeation of O ₂ and H ₂ O Decrease in electrical conductivity and molecular weight of PMA	Yeh et al. (2007)
PANI-Na-MMT PANI-O-MMT	PANI-MMT in NMP/CRS/1 M H ₂ SO ₄ 3.5 wt% NaCl	In situ chemical polymerization in the presence of APS, HCl	FTIR, four-probe technique, potentiodynamic polarization, cyclic voltammetry	Higher electrical conductivity for PANI-O-MMT Better anticorrosion performance only in 3.5 wt% NaCl	Olad and Rashidzadeh (2008)
PANI-O-MMT	PANI-MMT (2 wt%) in ethyl silicate ZRP/carbon steel/3.5 wt% NaCl	Suspension polymerization in the presence of APS	FTIR, XRD, SEM, four-probe technique, OCP monitoring, EIS	Higher electrical conductivity for PANI-O-MMT and lower for PANI-Na-MMT compared to PANI Better anticorrosion performance	Akbarinezhad et al. (2011)

Table 3 continued

Nanocomposite	Coating composition/substrate/corrosive medium	Synthesis method	Coating characterization	Salient features	References
PANI-Na-MMT	DBSA-doped PANI-Na-MMT/C45 steel/3.5 wt% NaCl	Solvent-free mechanochemical intercalation method	FTIR, UV–vis, SEM, potentiodynamic polarization, EIS	Porous network-type morphology Superior in corrosion protection over neat PANI coatings	Kalaivasan and Shafi (2012)
PANI-Na-MMT	HCl-doped PANI-Na-MMT/C45 steel/3.5 wt% NaCl	Solvent-free mechanochemical intercalation method	FTIR, XRD, SEM, potentiodynamic polarization	Superior in corrosion protection over neat PANI coatings	Kalaivasan (2015)
PANI-Na-MMT PANI-O-MMT	PANI-Na-MMT(2 wt%) in epoxy/Fe/3.5wt% NaCl	In situ chemical polymerization in the presence of APS, HCl	FTIR, XRD, potentiodynamic polarization, EIS, adhesion tests	Higher anticorrosion efficiency for PANI-O-MMT Improved adhesion strength	Navarchian et al. (2014)
PANI-Clino	PMA-Clino in NMP/Fe/ 1 M H ₂ SO ₄ 1 M HCl 3.5 wt% NaCl	In situ chemical polymerization in the presence of APS, HCl (1, 3, 5 wt% Clino)	FTIR, XRD, SEM, cyclic voltammetry, potentiodynamic polarization	Corrosion protection efficiency depends on the corrosive medium Higher anticorrosion efficiency at 3 wt% loading	Olad and Naseri (2010)
PANI-AD-LDH	PANI-AD-LDH(5 wt%) in epoxy/mild steel/3.5 wt% NaCl	In situ chemical polymerization in the presence of APS, HCl after the V ₁₀ O ₂₈ ⁶⁻ intercalation	FTIR, XRD, SEM, TGA, potentiodynamic polarization, salt spray test, OCP monitoring, EIS	Enhancement of corrosion protection properties in NaCl Short nanorods Partial exfoliation of AD-LDH in the PANI matrix	Hu et al. (2014)

Table 4 Nanocomposites of PANI with carbon-based materials

Nanocomposite	Coating composition/substrate/corrosive medium	Synthesis method	Coating characterization	Salient features	References
PANI-graphene	PANI-graphene in NMP/steel/ 3.5wt% NaCl	In situ chemical polymerization using functionalized graphene, APS, HCl	FTIR, TEM, TGA, four-probe technique, potentiodynamic polarization, gas permeability analysis	Well-dispersed graphene in PANI, high aspect ratio Enhanced impermeability for O ₂ and H ₂ O	Chang et al. (2012)
PANI-CNTs	PANI-CNTs/AISI 304/50 mM H ₂ SO ₄	Cyclic voltammetry form ANI, H ₂ SO ₄ solution	Cyclic voltammetry, SEM, in situ FTIR spectra	CNTs affect the electronic structure of PANI Nano-fibrillar morphology Blocking of ferrous ions	Martina et al. (2011)

Table 4 continued

Nanocomposite	Coating composition/substrate/corrosive medium	Synthesis method	Coating characterization	Salient features	References
PANI-MWCNTs	PANI-MWCNTs in epoxy/steel/3.5wt% NaCl	In situ chemical polymerization in presence of APS, HCl	Potentiodynamic polarization OCP monitoring, EIS	Lower corrosion rate than that of epoxy-coated steel Protection for 120 h of immersion	Deshpande et al. (2013)
PANI-MWCNTs	PANI-f-CNTs/mild steel/3.5 wt% NaCl	In situ chemical polymerization in presence of APS	Raman, IR, UV-Vis, SEM, TGA, dynamic hardness, adhesion strength, EIS,	Uniform fibrous morphology Improved mechanical strength Strong interfacial interactions between PANI and f-CNT	Kumar and Gasem (2015a)
PANI-MWCNTs	PANI-f-CNTs/mild steel/3.5 wt% NaCl	Cyclic voltammetry from ANI, oxalic acid, SDS	IR, UV-Vis, SEM, TGA, EIS dynamic hardness, cyclic voltammetry, contact angle, potentiodynamic polarization	Uniform dispersion of f-CNTs in PANI matrix Increasing hydrophobic character with f-CNT content	Kumar and Gasem (2015b)

References

- Abaci S, Nessark B (2015) Characterization and corrosion protection properties of composite material (PANI + TiO₂) coatings on A304 stainless steel. *J Coat Technol Res* 12:107–120. doi:10.1007/s11998-014-9611-x
- Abaci S, Nessark B, Riahi F (2014) Preparation and characterization of polyaniline + TiO₂ composite films. *Ionics* 20:1693–1702. doi:10.1007/s11581-014-1129-9
- Abu-Thabit NY, Makhlof ASH (2014) Recent advances in polyaniline (PANI)-based organic coatings for corrosion protection. In: Makhlof ASH (ed) *Handbook of smart coatings for materials protection*. Woodhead Publishing Ltd, U.K., pp 459–486
- Akbarinezhad E, Ebrahimi M, Sharif F, Attar MM, Faridi HR (2011) Synthesis and evaluating corrosion protection effects of emeraldine base PANi/clay nanocomposite as a barrier pigment in zinc-rich ethyl silicate primer. *Prog Org Coat* 70:39–44. doi:10.1016/j.porgcoat.2010.09.016
- Alam J, Riaz U, Ashraf SM, Ahmad S (2008) Corrosion protective performance of nano polyaniline/ferrite dispersed alkyl coatings. *J Coat Tech Res* 5:123–128
- Alam J, Riaz U, Ahmad S (2009) High performance corrosion resistant polyaniline/alkyd ecofriendly coatings. *Curr Appl Phys* 9:80–86. doi:10.1016/j.cap.2007.11.015
- Alam J, Kashif M, Ahmad S, Mohammad AW (2010) Electrochemical corrosion protection studies Pani/Ferrite/Alkyd nano composite coating. *World Appl Sci J* 9:01–05
- Alam M, Akram D, Sharmin E, Zafar F, Ahmad S (2014) Vegetable oil based eco-friendly coating materials: a review article. *Arab J Chem* 7:469–479. doi:10.1016/j.arabjc.2013.12.023
- Alam R, Mobin M, Aslam J (2016) Investigation of anti-corrosive properties of poly(aniline-co-2-pyridylamine-co-2,3-xylylidine) and its nanocomposite poly(aniline-co-2-pyridylamine-co-2,3-xylylidine)/ZnO on mild steel in 0.1 M HCl. *Appl Surf Sci* 368:360–367
- Alvi F, Ram MK, Gomez H, Joshi RK, Kumar A (2010) Evaluating the chemio-physio properties of novel zinc oxide-polyaniline nanocomposite polymer films. *Polym J* 42:935–940. doi:10.1038/pj.2010.89
- Alvi F, Aslam N, Shaukat SF (2015) Corrosion inhibition study of zinc oxide-polyaniline nanocomposite for aluminum and steel. *Am J Appl Chem* 3:57–64
- Anoop KS, Bhandari H, Sharma C, Khatoon F, Dhawan SK (2013) A new smart coating of polyaniline-SiO₂ composite for protection of mild steel against corrosion in strong acidic medium. *Polym Int* 62:1192–1201
- Ates M (2016) A review on conducting polymer coatings for corrosion protection. *J Adhes Sci Technol* 30:1510–1536
- Ates M, Topkaya E (2015) Nanocomposite film formations of polyaniline via TiO₂, Ag, and Zn, and their corrosion protection properties. *Prog Org Coat* 82:33–40
- Bagherzadeh MR, Mousavinejad T (2012) Preparation and investigation of anticorrosion properties of the water-based epoxy-clay nanocoating modified by Na⁺-MMT and Cloisite 30B. *Prog Org Coat* 74:589–595
- Baibarac M, Gomez-Romero P (2006) Nanocomposites based on conducting polymers and carbon nanotubes from fancy materials to functional applications. *J Nanosci Nanotechnol* 6:1–14
- Beard BC, Spellane P (1997) XPS evidence of redox chemistry between cold rolled steel and polyaniline. *Chem Mater* 9:1949–1953. doi:10.1021/Cm960256x

- Behzadnasab M, Mirabedini SM, Kabiri K, Jamali S (2011) Corrosion performance of epoxy coatings containing silane treated ZrO_2 on mild steel in 3.5% NaCl solution. *Corros Sci* 53:89–98
- Bhandari H, Anoop Kumar S, Dhawan SK (eds) (2012) Conducting polymer nanocomposites for anticorrosive and antistatic applications. INTECHOPEN.COM: INTECH
- Biallozor S, Kupniewska A (2005) Conducting polymers electrodeposited on active metals. *Synth Met* 155:443–449. doi:10.1016/j.synthmet.2005.09.002
- Brodinove J, Stejskai J, Kalendova A (2007) Investigation of ferrites properties with polyaniline layer in anticorrosive coatings. *J Phys Chem Sol* 68:1091–1095
- Cecchetto L, Ambat R, Davenport AJ, Delabouglise D, Petit JP, Neel O (2007) Emeraldine base as corrosion protective layer on aluminium alloy AA5182, effect of the surface microstructure. *Corros Sci* 49:818–829. doi:10.1016/j.corsci.2006.06.012
- Chang K-C, Lai M-C, Peng C-W, Chen Y-T, Yeh J-M, Lin C-L, Yang J-C (2006) Comparative studies on the corrosion protection effect of DBSA-doped polyaniline prepared from in situ emulsion polymerization in the presence of hydrophilic Na^+ -MMT and organophilic organo-MMT clay platelets. *Electrochim Acta* 51:5645–5653
- Chang C-H, Jang GW, Peng CW, Lin CY, Shieh JC, Yeh JM, Li WT (2007) Comparatively electrochemical studies at different operational temperatures for the effect of nanoclay platelets on the anticorrosion efficiency of DBSA-doped polyaniline/ Na^+ -MMT clay nanocomposite coatings. *Electrochim Acta* 52:5191–5200
- Chang C-H, Huang T-C, Peng C-W, Yeh T-C, Lu H-I, Hung W-I, Yeh J-M (2012) Novel anticorrosion coatings prepared from polyaniline/graphene composites. *Carbon* 50:5044–5051. doi:10.1016/j.carbon.2012.06.043
- Chaudhari S, Patil PP, Mandale AB, Patil KR, Sainkar SR (2007) Use of poly(o-toluidine)/ ZrO_2 nanocomposite coatings for the corrosion protection of mild steel. *J Appl Polym Sci* 106:220–229
- Chaudhari S, Gaikwad AB, Patil PP (2010) Synthesis and corrosion protection aspects of poly(o-toluidine)/CdO nanoparticle composite coatings on mild steel. *J Coat Technol Res* 7:119–129
- Chiou NR, Epstein AJ (2005a) Polyaniline nanofibers prepared by dilute polymerization. *Adv Mater* 17:1679–1683. doi:10.1002/adma.200401000
- Chiou NR, Epstein AJ (2005b) A simple approach to control the growth of polyaniline nanofibers. *Synth Met* 153:69–72. doi:10.1016/j.synthmet.2005.07.145
- Choi EK, Jeon IY, Oh SJ, Baek JB (2010) “Direct” grafting of linear macromolecular “wedges” to the edge of pristine graphite to prepare edge-functionalized graphene-based polymer composites. *J Mater Chem* 20:10936–10942
- Ciric-Marjanovic G (2013) Recent advances in polyaniline research: polymerization mechanisms, structural aspects, properties and applications. *Synth Met* 177:1–47
- Ćirić-Marjanović G (2013) Recent advances in polyaniline composites with metals, metalloids and nonmetals. *Synth Met* 170:31–56. doi:10.1016/j.synthmet.2013.02.028
- Compton OC, Kim S, Pierre C, Torkelson JM, Nguyen ST (2010) Crumpled graphene nanosheets as highly effective barrier property enhancers. *Adv Mater* 22:4759–4763. doi:10.1002/adma.201000960
- De Riccardis MF, Martina V (2014) Hybrid conducting nanocomposites coatings for corrosion protection In: Aliofkhaezrai M (Ed), *Developments in corrosion protection*, INTECH
- DeBerry DW (1985) Modification of the electrochemical and corrosion behavior of stainless steels with an electroactive coating. *J Electrochem Soc* 132:1022–1026
- Deshpande PP, Sazou D (2015) Corrosion protection by intrinsically conducting polymers. CRC Press, Boca Raton, FL
- Deshpande PP, Vathare SS, Vagge ST, Tomšik E, Stejskal J (2013) Conducting polyaniline—multi-wall carbon nanotubes composite paints for corrosion protection: electrochemical investigations. *Chem Paper* 67:1072–1078
- Deshpande PP, Jadhav NG, Gelling VJ, Sazou D (2014) Conducting polymers for corrosion protection: a review. *J Coat Technol Res* 11:473–494
- Do Nascimento GM, Constantino VRL, Landers R, Temperini MLA (2006) Spectroscopic characterization of polyaniline formed in the presence of montmorillonite clay. *Polymer* 47:6131–6139
- Dominis AJ, Spinks GM, Wallace GG (2003) Comparison of polyaniline primers prepared with different dopants for corrosion protection of steel. *Prog Org Coat* 48(1):43–49. doi:10.1016/S0300-9440(03)00111-5
- Elkais AR, Gvozdenović MM, Jugović BZ, Grgur BN (2013) The influence of thin benzoate-doped polyaniline coatings on corrosion protection of mild steel in different environments. *Prog Org Coat* 76:670–676. doi:10.1016/j.porgcoat.2012.12.008
- Eskizeybek V, Sari F, Gulce H, Gulce A, Avci A (2012) Preparation of the new polyaniline/ZnO nanocomposite and its photocatalytic activity for degradation of methylene blue and malachite green dyes under UV and natural sun lights irradiations. *Appl Catal B Environm* 119:197–206. doi:10.1016/j.apcatb.2012.02.034
- Fang J, Xu K, Zhu LH, Zhou ZX, Tang HQ (2007) A study on mechanism of corrosion protection of polyaniline coating and its failure. *Corros Sci* 49:4232–4242. doi:10.1016/j.corsci.2007.05.017
- Ganash A (2014) Anticorrosive properties of poly(o-phenylenediamine)/ZnO nanocomposites coated stainless steel. *J Nanomater* 2014, Article ID 540276, 540278 pp
- Gangopadhyay R, De A (2000) Conducting polymer nanocomposites: a brief overview. *Chem Mater* 12:608–622
- Gu J, Ma L, Gan M, Zhang F, Li W, Huang C (2012) Preparation and thermal properties of Poly(2,3-dimethylaniline)/ ZrO_2 composite. *Thermochim Acta* 549:13–16. doi:10.1016/j.tca.2012.09.004
- Hosseini MG, Jafari M, Najjar R (2011) Effect of polyaniline-montmorillonite nanocomposite powders addition on corrosion performance of epoxy coatings on Al 5000. *Surf Coat Technol* 206:280–286. doi:10.1016/j.surfcoat.2011.07.012
- Hu J, Gan M, Ma L, Li Z, Yan J, Zhang J (2014) Synthesis and anticorrosive properties of polymer-clay nanocomposites via chemical grafting of polyaniline onto Zn–Al layered double hydroxides. *Surf Coat Technol* 240:55–62. doi:10.1016/j.surfcoat.2013.12.012
- Hu CB, Zheng YS, Ding YS, Ma BY, Li Y (2016) Preparation of polyaniline/nano SiC/epoxy hybrid coating and evaluation of its corrosion resistant property. *J Polym Mater* 33:1–15
- Huang JW, Hu CB, Qing YQ (2015) Preparation and corrosion resistance of poly(o-toluidine)/nano SiC/epoxy composite coating. *Int J Electrochem Sci* 10:10607–10618
- Jafari Y, Shabani-Nooshabadi M, Ghoreishia SM (2013) Electropolymerized coatings of poly(o-anisidine) and poly(o-anisidine)- TiO_2 nanocomposite on aluminum alloy 3004 by using the galvanostatic method and their corrosion protection performance. *Polym Adv Technol* 25:279–287
- Jafari Y, Ghoreishi SM, Shabani-Nooshabadi M (2016) Polyaniline/Graphene nanocomposite coatings on copper: electropolymerization, characterization, and evaluation of corrosion protection performance. *Synth Met* 217:220–230
- Kalaivasan N (2015) Corrosion protection aspects of mechanochemically synthesized polyaniline/MMT clay nanocomposites. *Res J Pharm Biol Chem Sci* 6:1301–1307
- Kalaivasan N, Syed Shafi S (2012) Enhancement of corrosion protection effect in mechanochemically synthesized polyaniline/

- MMT clay nanocomposites. Arab J Chem. doi:10.1016/j.arabjc.2012.06.018
- Kalendova A, Vesely D, Stejskal J (2008) Organic coatings containing polyaniline and inorganic pigments as corrosion inhibitors. Prog Org Coat 62:105–116. doi:10.1016/j.porgcoat.2007.10.001
- Karpakam V, Kamaraj K, Sathiyarayanan S (2011) Electrosynthesis of PANI-Nano TiO₂ composite coating on steel and its anti-corrosion performance. J Electrochem Soc 158:C416–C423. doi:10.1149/2.023112jes
- Kendig M, Hon M (2004) Environmentally triggered release of oxygen-reduction inhibitors from inherently conducting polymers. Corrosion 60:1024–1030
- Kendig M, Hon M, Warren L (2003) ‘Smart’ corrosion inhibiting coatings. Prog Org Coat 47:183–189
- Khan MI, Chaudhry AU, Hashim S, Zahoor MK, Iqbal MZ (2010) Recent developments in intrinsically conductive polymer coatings for corrosion protection [Review]. Chem Eng Res Bull 14:73–86
- Kinlen PJ, Ding Y, Silverman DC (2002) Corrosion protection of mild steel using sulfonic and phosphonic acid-doped polyanilines. Corrosion 58:490–497
- Konyushenko EN, Stejskal J, Trchova M, Hradil J, Kovářová J, Prokeš J, Sapurina I (2006) Multi-wall carbon nanotubes coated with polyaniline. Polymer 47:5715–5723
- Kumar AM, Gasem ZM (2015a) Effect of functionalization of carbon nanotubes on mechanical and electrochemical behavior of polyaniline nanocomposite coatings. Surf Coat Technol 276:416–423. doi:10.1016/j.surfcoat.2015.06.036
- Kumar AM, Gasem ZM (2015b) In situ electrochemical synthesis of polyaniline/f-MWCNT nanocomposite coatings on mild steel for corrosion protection in 3.5% NaCl solution. Prog Org Coat 78:387–394
- Li Y, Wang X (2012) Intrinsically conducting polymers and their composites for anticorrosion and antistatic applications. In: Yang X (ed) Semiconducting polymer composites: principles, morphologies, properties and applications. Wilvy-VCH Verlag GmbH & Co. KGaA, Weinheim, pp 269–298
- Li Y, Zhang H, Wang X, Li J, Wang F (2011) Role of dissolved oxygen diffusion in coating defect protection by emeraldine base. Synth Met 161:2312–2317
- Li G, Li Y, Peng H, Qin Y (2013a) Synthesis and electrochemical performances of dispersible polyaniline/sulfonated graphene composite nanosheets. Synth Met 184:10–15
- Li Z, Ma L, Gan M, Qiu W, Fu D, Li S, Bai Y (2013b) Synthesis and anticorrosion performance of poly(2,3-dimethylaniline)-TiO₂ composite. Prog Org Coat 76:1161–1167. doi:10.1016/j.porgcoat.2013.03.012
- Ma L, Chen F, Li Z, Gan M, Yan J, Wei S, Zeng J (2014) Preparation and anticorrosion property of poly(2,3-dimethylaniline) modified by nano-SiO₂. Compos B Eng 58:54–58. doi:10.1016/j.compositesb.2013.10.064
- Mahajan LH, Mhaske ST (2012) Composite microspheres of poly(o-anisidine)/TiO₂. Mater Lett 68:183–186. doi:10.1016/j.matlet.2011.10.025
- Mahulikar PP, Jadhav RS, Hundiwal DG (2011) Performance of polyaniline/TiO₂ nanocomposites in epoxy for corrosion resistant coatings. Iran Polym J 20:367–376
- Martina V, De Riccardis MF, Carbone D, Rotolo P, Bozzini B, Mele C (2011) Electrodeposition of polyaniline-carbon nanotubes composite films and investigation on their role in corrosion protection of austenitic stainless steel by SNIFTIR analysis. J Nanopart Res 13:6035–6047
- Mostafaei A, Nasirpour F (2013) Electrochemical study of epoxy coating containing novel conducting nanocomposite comprising polyaniline-ZnO nanorods on low carbon steel. Corros Eng Sci Technol 48:513–524. doi:10.1179/1743278213Y.0000000084
- Mostafaei A, Nasirpour F (2014) Epoxy/polyaniline-ZnO nanorods hybrid nanocomposite coatings: synthesis, characterization and corrosion protection performance of conducting paints. Prog Org Coat 77:146–159. doi:10.1016/j.porgcoat.2013.08.015
- Mostafaei A, Zolriasatein A (2012) Synthesis and characterization of conducting polyaniline nanocomposites containing ZnO nanorods. Prog Natl Sci: Mater Int 22:273–280. doi:10.1016/j.pnsc.2012.07.002
- Navarchian AH, Joulazadeh M, Karimi F (2014) Investigation of corrosion protection performance of epoxy coatings modified by polyaniline/clay nanocomposites on steel surfaces. Prog Org Coat 77:347–353. doi:10.1016/j.porgcoat.2013.10.008
- Nghia ND, Tung NT (2009) Study on synthesis and anticorrosion properties of polymer nanocomposites based on super paramagnetic Fe₂O₃-NiO nanoparticle and polyaniline. Synth Met 159:831–834
- Nguyen TN, Nguyen TA, Pham MC, Piro B, Normand B, Takenouti H (2004) Mechanism for protection of iron corrosion by an intrinsically electronic conducting polymer. J Electroanal Chem 572:225–234
- Oh SG, Im SS (2002) Electroconductive polymer nanoparticles preparation and characterization of PANI and PEDOT nanoparticles. Curr Appl Phys 2:273–277
- Olad A, Naseri B (2010) Preparation, characterization and anticorrosive properties of a novel polyaniline/clinoptilolite nanocomposite. Prog Org Coat 67:233–238. doi:10.1016/j.porgcoat.2009.12.003
- Olad A, Nosrati R (2013) Preparation and corrosion resistance of nanostructured PVC/ZnO-polyaniline hybrid coating. Prog Org Coat 76:113–118. doi:10.1016/j.porgcoat.2012.08.017
- Olad A, Rashidzadeh A (2008) Preparation and anticorrosive properties of PANI/Na-MMT and PANI/O-MMT nanocomposites. Prog Org Coat 62:293–298
- Olad A, Rasouli H (2010) Enhanced corrosion protective coating based on conducting polyaniline/zinc nanocomposite. J Appl Polym Sci 115:2221–2227. doi:10.1002/App.31320
- Olad A, Barati M, Shirmohammadi H (2011) Conductivity and anticorrosion performance of polyaniline/zinc composites: investigation of zinc particle size and distribution effect. Prog Org Coat 72:599–604. doi:10.1016/j.porgcoat.2011.06.022
- Olad A, Barati M, Behboudi S (2012) Preparation of PANI/epoxy/Zn nanocomposite using Zn nanoparticles and epoxy resin as additives and investigation of its corrosion protection behavior on iron. Prog Org Coat 74:221–227. doi:10.1016/j.porgcoat.2011.12.012
- Patil RC, Radhakrishnan S (2006) Conducting polymer based hybrid nano-composites for enhanced corrosion protective coatings. Prog Org Coat 57:332–336
- Pud A, Orgutsov N, Korzhenko A, Shapoval G (2003) Some aspects of preparation methods and properties of polyaniline blends and composites with organic polymers. Prog Polym Sci 28:1701–1753
- Radhakrishnan S, Siju CR, Mahanta D, Patil S, Madras G (2009) Conducting polyaniline-nano-TiO₂ composites for smart corrosion resistant coatings. Electrochim Acta 54:1249–1254
- Reena VL, Sudha JD, Pavithran C (2009) Role of amphiphilic dopants on the shape and properties of electrically conducting polyaniline-clay nanocomposite. J Appl Polym Sci 113:4066–4076. doi:10.1002/app.30525
- Reijnders L (2009) The release of TiO₂ and SiO₂ nanoparticles from nanocomposites. Polym Degrad Stab 94:873–876
- Rohwerder M (2009) Conducting polymers for corrosion protection: a review. Int J Mater Res 100:1331–1342. doi:10.3139/146.110205
- Samui AB, Patankar AS, Rangarajan J, Deb PC (2003) Study of polyaniline containing paint for corrosion prevention. Prog Org Coat 47:1–7. doi:10.1016/S0300-9440(02)00117-0

- Sarkar N, Sahoo G, Das R, Prusty G, Sahu D, Swain SK (2016) Anticorrosion performance of three-dimensional hierarchical PANI@BN nanohybrids. *Ind Eng Chem Res* 55:2921–2931. doi:10.1021/acs.iecr.5b04887
- Sathiyarayanan S, Azim SS, Venkatachari G (2007a) Corrosion protection of magnesium ZM 21 alloy with polyaniline-TiO₂ composite containing coatings. *Prog Org Coat* 59:291–296. doi:10.1016/j.porgcoat.2007.04.004
- Sathiyarayanan S, Azim SS, Venkatachari G (2007b) A new corrosion protection coating with polyaniline-TiO₂ composite for steel. *Electrochim Acta* 52:2068–2074
- Sathiyarayanan S, Azim SS, Venkatachari G (2007c) Preparation of polyaniline-Fe₂O₃ composite and its anticorrosion performance. *Synth Met* 157:751–757
- Sathiyarayanan S, Azim SS, Venkatachari G (2007d) Preparation of polyaniline-TiO₂ composite and its comparative corrosion protection performance with polyaniline. *Synth Met* 157:205–213
- Sathiyarayanan S, Maruthan K, Muthukrishnan S, Venkatachari G (2009) High performance polyaniline containing coating system for wet surfaces. *Prog Org Coat* 66:113–117
- Sazou D (2001) Electrodeposition of ring-substituted polyanilines on Fe surfaces from aqueous oxalic acid solutions and corrosion protection of Fe. *Synth Met* 118:133–147
- Sazou D, Georgolios C (1997) Formation of conducting polyaniline coatings on iron surfaces by electropolymerization of aniline in aqueous solutions. *J Electroanal Chem* 429:81–93
- Sazou D, Kourouzidou M, Pavlidou E (2007) Potentiodynamic and potentiostatic deposition of polyaniline on stainless steel: electrochemical and structural studies for a potential application to corrosion control. *Electrochim Acta* 52:4385–4397. doi:10.1016/j.electacta.2006.12.020
- Sen T, Mishra S, Shimpi NG (2016) Synthesis and sensing applications of polyaniline nanocomposites: a review. *RSC Adv* 6:42196–42222. doi:10.1039/c6ra03049a
- Shabani-Nooshabadi M, Karimian-Taheria F (2015) Electrosynthesis of a polyaniline/zeolite nanocomposite coating on copper in a three-step process and the effect of current density on its corrosion protection performance. *RSC Adv* 5:96601–96610. doi:10.1039/C5RA14333K
- Shabani-Nooshabadi M, Ghoreishi SM, Behpour M (2011) Direct electrosynthesis of polyaniline-montmorillonite nanocomposite coatings on aluminum alloy 3004 and their corrosion protection performance. *Corros Sci* 53:3035–3042. doi:10.1016/j.corsci.2011.05.053
- Silva JEP, Torresi SIC, Torresi RM (2005) Polyaniline acrylic coatings for corrosion inhibition: the role played by counter-ions. *Corros Sci* 47:811–822
- Silva JEP, Torresi SIC, Torresi RM (2007) Polyaniline/poly(methyl-methacrylate) blends for corrosion protection: the effect of passivating dopants on different metals. *Prog Org Coat* 58:33–39
- Singh BP, Jena BK, Bhattacharjee S, Besra L (2013a) Development of oxidation and corrosion resistance hydrophobic graphene oxide-polymer composite coating on copper. *Surf Coat Technol* 232:475–481. doi:10.1016/j.surfcoat.2013.06.004
- Singh BP, Nayak S, Nanda KK, Jena BK, Bhattacharjee S, Besra L (2013b) The production of a corrosion resistant graphene reinforced composite coating on copper by electrophoretic deposition. *Carbon* 6:47–56. doi:10.1016/j.carbon.2013.04.063
- Somani PR, Marimuthu R, Mulik UP, Sainkar SR, Amalnerkar DP (1999) High piezoresistivity and its origin in conducting polyaniline/TiO₂ composites. *Synth Met* 106:45–52. doi:10.1016/S0379-6779(99)00081-8
- Soundararajah QY, Karunaratne BSB, Rajapakse RMG (2009) Montmorillonite polyaniline nanocomposites: preparation, characterization and investigation of mechanical properties. *Mater Chem Phys* 113:850–855
- Souza S (2007) Smart coating based on polyaniline acrylic blend for corrosion protection of different metals. *Surf Coat Technol* 201:7574–7581
- Souza S, Silva JEP, Torresi SIC, Temperini MLA, Torresi RM (2001) Polyaniline based acrylic blends for iron corrosion protection. *Electrochim Solid State Lett* 4:B27–B30
- Spinks GM, Dominis AJ, Wallace GG, Tallman DE (2002) Electroactive conducting polymers for corrosion control—Part 2. Ferrous metals. *J Solid State Electrochem* 6:85–100. doi:10.1007/s100080100211
- Su L, Gan YX (2012) Experimental study on synthesizing TiO₂ nanotube/polyaniline (PANI) nanocomposites and their thermoelectric and photosensitive property characterization. *Compos Part B Eng* 43:170–182. doi:10.1016/j.compositesb.2011.07.015
- Sui JH, Cai W (2006) Formation of ZrO₂ coating on the NiTi alloys for improving their surface properties. *Nucl Instrum Methods Phys Res B* 251:402–406
- Tallman DE, Spinks G, Dominis A, Wallace GG (2002) Electroactive conducting polymers for corrosion control Part 1. General introduction and a review of non-ferrous metals. *J Solid State Electrochem* 6:73–84. doi:10.1007/s100080100212
- Torresi RM, Souza S, Silva JEP, Torresi SIC (2005) Galvanic coupling between metal substrate and polyaniline acrylic blends: corrosion protection mechanism. *Electrochim Acta* 50:2213–2218
- Tuken T, Yazici B, Erbil M (2006) Zinc modified polyaniline coating for mild steel protection. *Mater Chem Phys* 99:459–464
- Weng C-J, Chen Y-L, Jhuo Y-S, Lin Y-L, Yeh J-M (2012) Advanced antistatic/anticorrosion coatings prepared from polystyrene composites incorporating dodecylbenzenesulfonic acid-doped SiO₂@polyaniline core-shell microspheres. *Polym Int* 62:774–782. doi:10.1002/pi.4362
- Wessling B (1996) Corrosion prevention with an organic metal (polyaniline): surface ennobling, passivation, corrosion test results. *Mater Corros* 47:439–445
- Xu J-C, Liu W-M, Li H-L (2005) Titanium dioxide doped polyaniline. *Mater Sci Eng C* 25:444–447
- Yavuz AG, Aysegul G (2007) Preparation of TiO₂/PANI composites in the presence of surfactants and investigation of electrical properties. *Synth Met* 157:235–242
- Yeh J-M, Liou SJ, Lai C-Y, Wu P-C (2001) Enhancement of corrosion protection effect in polyaniline via the formation of polyaniline-clay nanocomposite materials. *Chem Mater* 13:1131–1136
- Yeh J-M, Chen C-L, Chen Y-C, Ma C-Y, Lee K-R, Wei Y, Li S (2002) Enhancement of corrosion protection effect of poly(o-ethoxyaniline) via the formation of poly(o-ethoxyaniline)-clay nanocomposite materials. *Polymer* 43:2729–2736
- Yeh J-M, Kuo T-H, Huang H-J, Chang K-C, Chang M-Y, Yang J-C (2007) Preparation and characterization of poly(o-methoxyaniline)/Na⁺-MMT clay nanocomposite via emulsion polymerization: electrochemical studies of corrosion protection. *Eur Polym J* 43:1624–1634
- Yu Q, Xu J, Liu J, Li B, Liu Y, Han Y (2012) Synthesis and properties of PANI/SiO₂ organic-inorganic hybrid films. *Appl Surf Sci* 263:532–535. doi:10.1016/j.apsusc.2012.09.100
- Zhang Y, Shao Y, Zhang T, Meng G, Wang F (2013) High corrosion protection of a polyaniline/organophilic montmorillonite coating for magnesium alloys. *Prog Org Coat* 76(5):804–811